Aerospace Science and Technology 25 (2013) 161–176

Contents lists available at SciVerse ScienceDirect

Aerospace Science and Technology

www.elsevier.com/locate/aescte

Analytical solution to optimal relocation of satellite formation flying in arbitrary elliptic orbits

Hancheol Cho, Sang-Young Park*, Sung-Moon Yoo, Kyu-Hong Choi

Astrodynamics & Control Lab., Dept. of Astronomy, Yonsei University, Seoul 120-749, Republic of Korea

ARTICLE INFO

Article history:
Received 19 January 2008
Received in revised form 10 October 2010
Accepted 5 January 2012
Available online 9 January 2012

Keywords:
Satellite formation flying
Fuel-optimal reconfiguration
Elliptic orbits
Fourier series
Low-level thrust

ABSTRACT

The current paper presents and examines a general analytical solution to the optimal reconfiguration problem of satellite formation flying in an arbitrary elliptic orbit. The proposed approach does not use any simplifying assumptions regarding the eccentricity of the reference orbit. For the fuel optimal reconfiguration problem, continuous and variable low-thrust accelerations can be represented by the Fourier series and summed into closed-form solutions. Initial and final boundary conditions are used to establish the constraints on the thrust functions. The analytical solution can be implicated by the Fourier coefficients that minimize propellant usage during the maneuver. This solution is found that compares favorably with numerical simulations. Also, this analytical solution is very useful for designing a reconfiguration controller for satellite formation flying in a general elliptic orbit.

1. Introduction

In the future, advanced space applications will utilize formation flying technologies that involve multiple satellites. Therefore, satellite formation flying requires technology drawn from various research fields such as relative orbit determination, formation keeping, formation reconfiguration, relative attitude determination, relative attitude control, etc. Among these technologies, the current paper focuses on formation reconfiguration. To build a desired formation or to change a formation shape, it is necessary to relocate satellites into the desired relative positions between satellites. The reconfiguration of satellites is achieved by optimizing the thrust accelerations required. There has already been a variety of research dealing with the problem of minimum propellant transfers for satellite reconfigurations in formation flying. Most of solutions have been numerically obtained because this problem is highly nonlinear. To employ a distributed computational architecture, a hybrid optimization algorithm is developed for satellite formation reconfiguration [15]. As well, using the calculus of variations approach, the optimal reconfiguration trajectories are numerically determined [7]. An algorithm for the reconfiguration problem is presented based upon Hamilton–Jacobi–Bellman optimality to generate a set of maneuvers to move from an initial stable formation to a final stable formation [3]. A reconfiguration problem about an Earth–Sun libration point is solved by use of an algorithm with generating functions to provide two impulsive maneuvers [4]. Finding the numerical solutions is somewhat difficult because the necessary and optimality conditions must be numerically satisfied. However, analytic solutions would give insight into the feedback controller, and therefore would be easily exploited for formation flying, if they could be uncovered. For reconfiguration maneuvers of formation flying, an analytical two-impulse solution is proposed using Gauss's variational equations [12]. This algorithm is based on the circular reference orbit described by the Hill–Clohessy–Wiltshire (HCW) equations. An analytic solution has been published for the formation relocation of a satellite using continuous and variable thrust acceleration in order to adopt low-thrust maneuvers [8]. These analytic solutions are very useful in their application to formation maintenance and relocation. However, this analytic solution is limited to formation flying in only a circular or near-circular orbit because the HCW equations are used in [8]. The relative motions in satellite formation become a more realistic and complex problem when the non-zero eccentricity of reference orbit (i.e., a Chief satellite's orbit) is considered. Therefore, the current paper extends the previous results in [8] to the satellite formation relocation problem in a general elliptic orbit. The proposed approach does not use any simplifying assumptions regarding the eccentricity of the reference orbit. In particular, the current paper provides the first presentation of the explicit closed-form solutions to relocation of formation flying in an elliptic reference orbit ($e \neq 0$). The analytical method developed in this paper yields closed-forms of accelerations, closed-forms of position and velocity vectors and closed-form of performance index, for any formation reconfiguration. The analytical solutions can be applied for spacecraft formation reconfigurations in highly elliptic orbit such

* Corresponding author. Tel.: +82 2 2123 5687, fax: +82 2 392 7680.
E-mail addresses: narziss@yonsei.ac.kr (H. Cho), spark@galaxy.yonsei.ac.kr (S.-Y. Park), smyoo@galaxy.yonsei.ac.kr (S.-M. Yoo), khchoi@galaxy.yonsei.ac.kr (K.-H. Choi).

1270-9638/$ – see front matter
doi:10.1016/j.ast.2012.01.005

as the Magnetosphere Multiscale Mission (MMS) [16]. The analysis does not take account of orbital perturbations nor nonlinearity, because Tschauner–Hempel equations [11] are used in the current study.

In the control problem in the current paper, the relative dynamics in an elliptic reference orbit are used. The true anomaly of the satellite is also used as an independent variable for convenience. The out-of-orbital plane motion is decoupled from the in-plane motion, so it can be handled independently. Although the in-plane motion is much more complicated than the out-of-orbit plane motion, the procedure for deriving an in-plane solution is similar to that for the case of an out-of-plane solution. To derive the analytical solution to the optimal reconfiguration problem, the inhomogeneous solution and the particular solution should be analytically formulated. Initial and final positions and velocities of the Deputy satellites are calculated using Tschauner–Hempel equations [11] in order to establish the constraints on the thrust functions. These constraints can be incorporated into the performance index by introducing Lagrange multipliers. The analytical solution is formed by the magnitude and direction of thrust accelerations as a function of the true anomaly. It is assumed that there are no restrictions on the thrust vector, and a transfer time is chosen as a specific value. The satellites are assumed to have low-level thrusters in three orthogonal directions which correspond to the radial, in-track and cross-track directions, respectively. Thrusters are fired during a significant fraction of an orbital period throughout the maneuver. Any thruster acceleration can be represented by the infinite Fourier series. With Parseval's theorem, the Fourier series can be summed into a closed-form solution. Analytical optimal solutions can be derived by extremizing the performance index with respect to all of the Fourier coefficients. Then, the solution minimizes propellant usage for the reconfiguration of satellite formation. Performing the analytical solutions, the satellites can generate an optimal reconfiguration trajectory. The analytic solutions are valid for an arbitrary elliptic orbit satisfying $0 < e < 1$ as well as a circular orbit. The present paper describes thrust accelerations in closed-form for the optimal satellite relocation problem and the solution will be very useful for designing a controller for satellite formation flying in a general elliptic orbit.

2. Relative orbital dynamics in an elliptic orbit

In this section, we briefly show relative dynamics for an elliptic orbit. This also provides the necessary equations to be used. Since the satellites are moving in an elliptical orbit, we should use the Tschauner–Hempel equations instead of Hill's equations. These equations, which were first derived by Tschauner and Hempel [11], are as follows:

$$\begin{bmatrix}\ddot{x}\\ \ddot{y}\\ \ddot{z}\end{bmatrix} = -2\begin{bmatrix}0 & -\dot{\theta} & 0\\ \dot{\theta} & 0 & 0\\ 0 & 0 & 0\end{bmatrix}\begin{bmatrix}\dot{x}\\ \dot{y}\\ \dot{z}\end{bmatrix} - \begin{bmatrix}-\dot{\theta}^2 & 0 & 0\\ 0 & -\dot{\theta}^2 & 0\\ 0 & 0 & 0\end{bmatrix}\begin{bmatrix}x\\ y\\ z\end{bmatrix} - \begin{bmatrix}0 & -\ddot{\theta} & 0\\ \ddot{\theta} & 0 & 0\\ 0 & 0 & 0\end{bmatrix}\begin{bmatrix}x\\ y\\ z\end{bmatrix} + \frac{\rho(\theta)^3}{\Gamma^4}\begin{bmatrix}2x\\ -y\\ -z\end{bmatrix} + \begin{bmatrix}T_x\\ T_y\\ T_z\end{bmatrix} \quad (1)$$

where the $x(t)$ axis lies in the radial direction, the $y(t)$ axis is in the in-track direction, and the $z(t)$ axis along the orbital angular momentum vector completes a right-handed system (see Fig. 1), while the dot ($\dot{}$) represents the differentiation with respect to time (t). In addition, $\theta(t)$ and e refer to the true anomaly and the eccentricity of the Chief satellite, respectively. $\rho(\theta) \equiv 1 + e\cos\theta$ and $\Gamma \equiv L^{3/2}/GM$ are defined, where $L = R^2\dot{\theta}$ is the magnitude of the orbital angular momentum of the Chief satellite, G is the universal gravitational constant, and M is the mass of Earth. It is assumed that the thrust $[T_x(t), T_y(t), T_z(t)]^{\mathrm{T}}$ can be applied at

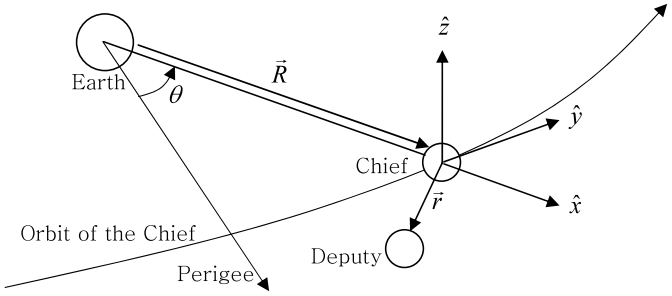

Fig. 1. The description of relative motion [14].

the desired directions during the maneuver. Changing the independent variable from time (t) to the true anomaly (θ), Eq. (1) can be rewritten as:

$$\begin{bmatrix}x\\ x'\\ y\\ y'\end{bmatrix}' = \begin{bmatrix}0 & 1 & 0 & 0\\ 1+2/\rho & -2\rho'/\rho & 2\rho'/\rho & 2\\ 0 & 0 & 0 & 1\\ -2\rho'/\rho & -2 & 1-1/\rho & -2\rho'/\rho\end{bmatrix}\begin{bmatrix}x\\ x'\\ y\\ y'\end{bmatrix} + \frac{\Gamma^4}{\rho^4}\begin{bmatrix}0 & 0\\ 1 & 0\\ 0 & 0\\ 0 & 1\end{bmatrix}\begin{bmatrix}T_x\\ T_y\end{bmatrix} \quad (2a)$$

$$\begin{bmatrix}z\\ z'\end{bmatrix}' = \begin{bmatrix}0 & 1\\ -1/\rho & -2\rho'/\rho\end{bmatrix}\begin{bmatrix}z\\ z'\end{bmatrix} + \frac{\Gamma^4}{\rho^4}\begin{bmatrix}0\\ 1\end{bmatrix}T_z \quad (2b)$$

where primer ($'$) represents differentiation with respect to the true anomaly, and thrust vector $\mathbf{T} = [T_x(\theta), T_y(\theta), T_z(\theta)]^{\mathrm{T}}$ and state vector $[x(\theta), y(\theta), z(\theta)]^{\mathrm{T}}$ are now described by the true anomaly. ρ, e, and Γ are the same as noted above, and $\rho' = -e\sin\theta$. The true anomaly (θ) is easily calculated from time using Kepler's equation. The in-plane ($x(\theta)$ and $y(\theta)$) motion and the out-of-plane ($z(\theta)$) motion are decoupled, so we can deal with the problems separately. Now, for brevity, let's consider the following transformation:

$$[\tilde{x}, \tilde{y}, \tilde{z}]^{\mathrm{T}} = \omega^{1/2}[x, y, z]^{\mathrm{T}} \quad (3)$$

$$\mathbf{u}(\theta) = \left[u_x(\theta), u_y(\theta), u_z(\theta)\right]^{\mathrm{T}} = \left[T_x(\theta), T_y(\theta), T_z(\theta)\right]^{\mathrm{T}}/\omega^{3/2} \quad (4)$$

where $\omega \equiv \dot{\theta}$, the orbital rate of the Chief satellite. With the same procedure as that derived by Humi [5], Eqs. (2a) and (2b) become very simple:

$$\begin{bmatrix}\tilde{x}\\ \tilde{x}'\\ \tilde{y}\\ \tilde{y}'\end{bmatrix}' = \begin{bmatrix}0 & 1 & 0 & 0\\ 3/\rho & 0 & 0 & 2\\ 0 & 0 & 0 & 1\\ 0 & -2 & 0 & 0\end{bmatrix}\begin{bmatrix}\tilde{x}\\ \tilde{x}'\\ \tilde{y}\\ \tilde{y}'\end{bmatrix} + \begin{bmatrix}0 & 0\\ 1 & 0\\ 0 & 0\\ 0 & 1\end{bmatrix}\begin{bmatrix}u_x\\ u_y\end{bmatrix} \quad (5a)$$

$$\begin{bmatrix}\tilde{z}\\ \tilde{z}'\end{bmatrix}' = \begin{bmatrix}0 & 1\\ -1 & 0\end{bmatrix}\begin{bmatrix}\tilde{z}\\ \tilde{z}'\end{bmatrix} + \begin{bmatrix}0\\ 1\end{bmatrix}u_z \quad (5b)$$

It is important to note that the actual position (x, y, z) and velocity $(\dot{x}, \dot{y}, \dot{z})$ are related to the pseudo-position $(\tilde{x}, \tilde{y}, \tilde{z})$ and pseudo-velocity $(\tilde{x}', \tilde{y}', \tilde{z}')$ as follows:

$$\begin{bmatrix}x(\theta)\\ y(\theta)\\ z(\theta)\end{bmatrix} = \frac{\Gamma}{\rho(\theta)}\begin{bmatrix}\tilde{x}(\theta)\\ \tilde{y}(\theta)\\ \tilde{z}(\theta)\end{bmatrix} \quad (6a)$$

$$\frac{\mathrm{d}}{\mathrm{d}t}\begin{bmatrix}x(\theta)\\ y(\theta)\\ z(\theta)\end{bmatrix} = \frac{e\sin\theta}{\Gamma}\begin{bmatrix}\tilde{x}(\theta)\\ \tilde{y}(\theta)\\ \tilde{z}(\theta)\end{bmatrix} + \frac{\rho(\theta)}{\Gamma}\begin{bmatrix}\tilde{x}'(\theta)\\ \tilde{y}'(\theta)\\ \tilde{z}'(\theta)\end{bmatrix} \quad (6b)$$

or

$$\begin{bmatrix} \tilde{x}(\theta) \\ \tilde{y}(\theta) \\ \tilde{z}(\theta) \end{bmatrix} = \frac{\rho(\theta)}{\Gamma} \begin{bmatrix} x(\theta) \\ y(\theta) \\ z(\theta) \end{bmatrix} \tag{7a}$$

$$\begin{bmatrix} \tilde{x}'(\theta) \\ \tilde{y}'(\theta) \\ \tilde{z}'(\theta) \end{bmatrix} = -\frac{e\sin\theta}{\Gamma} \begin{bmatrix} x(\theta) \\ y(\theta) \\ z(\theta) \end{bmatrix} + \frac{\Gamma}{\rho(\theta)} \frac{\mathrm{d}}{\mathrm{d}t} \begin{bmatrix} x(\theta) \\ y(\theta) \\ z(\theta) \end{bmatrix} \tag{7b}$$

3. Solutions to relative orbital dynamics in an elliptic orbit

In this section, we derive the solutions to relative orbital dynamics in an elliptic orbit. Eqs. (5a) and (5b) are key equations from which we start. Because the $\tilde{z}$ motion is less difficult to deal with, we will consider the out-of-plane maneuvers first.

3.1. Solution to out-of-plane maneuvers

Eq. (5b) is of the form:

$$\mathbf{Z}' = \mathbf{A_z Z} + \mathbf{B_z} u_z$$

As is well known, it has the following solution:

$$\begin{bmatrix} \tilde{z}(\theta) \\ \tilde{z}'(\theta) \end{bmatrix} = \boldsymbol{\Phi}_{\mathbf{z}}(\theta)\boldsymbol{\Phi}_{\mathbf{z}}^{-1}(\theta_0) \begin{bmatrix} \tilde{z}(\theta_0) \\ \tilde{z}'(\theta_0) \end{bmatrix} + \boldsymbol{\Phi}_{\mathbf{z}}(\theta) \int_{\theta_0}^{\theta} \boldsymbol{\Phi}_{\mathbf{z}}^{-1}(\tau) \begin{bmatrix} 0 \\ 1 \end{bmatrix} u_z(\tau)\,\mathrm{d}\tau \tag{8}$$

where $\boldsymbol{\Phi}_{\mathbf{z}}(\theta)$ is a fundamental matrix associated with $\mathbf{A_z} = \left[\begin{smallmatrix} 0 & 1 \\ -1 & 0 \end{smallmatrix}\right]$, and $\boldsymbol{\Phi}_{\mathbf{z}}(\theta)\boldsymbol{\Phi}_{\mathbf{z}}^{-1}(\theta_0)$ is the state transition matrix associated with $\mathbf{A_z}(\theta)$. θ_0 is the true anomaly when the thruster starts to fire, and τ is used as an integration variable. The first term on the right in Eq. (8) is a homogeneous solution, while the second is a particular solution which contains the thrust u_z. It is straightforward to show that

$$\boldsymbol{\Phi}_{\mathbf{z}}(\theta) = \begin{bmatrix} \cos\theta & \sin\theta \\ -\sin\theta & \cos\theta \end{bmatrix} \tag{9a}$$

$$\boldsymbol{\Phi}_{\mathbf{z}}^{-1}(\theta) = \begin{bmatrix} \cos\theta & -\sin\theta \\ \sin\theta & \cos\theta \end{bmatrix} \tag{9b}$$

Thus, the homogeneous solution to Eq. (5b) is

$$\begin{bmatrix} \hat{\tilde{z}}(\theta) \\ \hat{\tilde{z}}'(\theta) \end{bmatrix} = \begin{bmatrix} \cos(\theta-\theta_0) & \sin(\theta-\theta_0) \\ -\sin(\theta-\theta_0) & \cos(\theta-\theta_0) \end{bmatrix} \begin{bmatrix} \tilde{z}(\theta_0) \\ \tilde{z}'(\theta_0) \end{bmatrix} \tag{10a}$$

or

$$\begin{bmatrix} \hat{z}(\theta) \\ \dot{\hat{z}}(\theta) \end{bmatrix} = \begin{bmatrix} \frac{\cos(\theta-\theta_0)+e\cos\theta}{1+e\cos\theta} & \Gamma^2 \frac{\sin(\theta-\theta_0)}{(1+e\cos\theta)(1+e\cos\theta_0)} \\ -\frac{1}{\Gamma^2}[\sin(\theta-\theta_0)+e(\sin\theta-\sin\theta_0)] & \frac{\cos(\theta-\theta_0)+e\cos\theta_0}{1+e\cos\theta_0} \end{bmatrix} \times \begin{bmatrix} z(\theta_0) \\ \dot{z}(\theta_0) \end{bmatrix} \tag{10b}$$

where we use the carat to denote its state in the absence of thrust; be careful about the difference between the actual state (z) and pseudo-state ($\tilde{z}$). $\tilde{z}(\theta_0)$ and $\tilde{z}'(\theta_0)$ at θ_0 must be calculated from the actual values $z(\theta_0)$ and $\dot{z}(\theta_0)$ using Eqs. (7a) and (7b). Inserting $e = 0$ into Eq. (10b) yields only the homogeneous solution of Hill's equations.

The particular solution to Eq. (5b) is

$$\begin{aligned} \tilde{z}_p(\theta) &= \sin\theta \int_{\theta_0}^{\theta} u_z(\tau)\cos\tau\,\mathrm{d}\tau - \cos\theta \int_{\theta_0}^{\theta} u_z(\tau)\sin\tau\,\mathrm{d}\tau \\ &= \Gamma^3 \int_{\theta_0}^{\theta} \frac{\sin(\theta-\tau)}{\rho(\tau)^3} T_z(\tau)\,\mathrm{d}\tau \end{aligned} \tag{11a}$$

$$\begin{aligned} \tilde{z}_p'(\theta) &= \cos\theta \int_{\theta_0}^{\theta} u_z(\tau)\cos\tau\,\mathrm{d}\tau + \sin\theta \int_{\theta_0}^{\theta} u_z(\tau)\sin\tau\,\mathrm{d}\tau \\ &= \Gamma^3 \int_{\theta_0}^{\theta} \frac{\cos(\theta-\tau)}{\rho(\tau)^3} T_z(\tau)\,\mathrm{d}\tau \end{aligned} \tag{11b}$$

where the following identity is used:

$$u_z(\theta) = \frac{T_z(\theta)}{\omega^{3/2}} = \frac{\Gamma^3}{\rho(\theta)^3} T_z(\theta)$$

In summary, the z thruster fires at θ_0 and the satellite sweeps out $\Delta\vartheta$ during which the thruster fires continuously at a variable thrust magnitude; after this, it is located at $\theta = \theta_0 + \Delta\vartheta$ and its position and velocity can be obtained by adding the homogeneous solution to the particular solution:

$$\begin{bmatrix} \tilde{z}(\theta) \\ \tilde{z}'(\theta) \end{bmatrix} = \begin{bmatrix} \hat{\tilde{z}}(\theta) \\ \hat{\tilde{z}}'(\theta) \end{bmatrix} + \begin{bmatrix} \tilde{z}_p(\theta) \\ \tilde{z}_p'(\theta) \end{bmatrix}$$

or

$$\begin{bmatrix} z(\theta) \\ \dot{z}(\theta) \end{bmatrix} = \begin{bmatrix} \hat{z}(\theta) \\ \dot{\hat{z}}(\theta) \end{bmatrix} + \begin{bmatrix} z_p(\theta) \\ \dot{z}_p(\theta) \end{bmatrix}$$

When the Chief satellite arrives at a final true anomaly (θ_F), the thruster is turned off and the Deputy satellite is in the desired relative position. That is, $\tilde{z}(\theta_F)$ and $\tilde{z}'(\theta_F)$ (or $z(\theta_F)$ and $\dot{z}(\theta_F)$) are our predefined values, which give the constraints on the thrust function. Of course, they must be transformed from the actual position and velocity by Eqs. (7a) and (7b). Then,

$$\begin{bmatrix} \tilde{z}_p(\theta_F) \\ \tilde{z}_p'(\theta_F) \end{bmatrix} = \begin{bmatrix} \tilde{z}(\theta_F) \\ \tilde{z}'(\theta_F) \end{bmatrix} - \begin{bmatrix} \hat{\tilde{z}}(\theta_F) \\ \hat{\tilde{z}}'(\theta_F) \end{bmatrix}$$

where $\hat{\tilde{z}}(\theta_F)$ and $\hat{\tilde{z}}'(\theta_F)$ are the position and velocity at θ_F if the thrust has not been applied. We must find where the thrust $u_z(\theta)$ meets $\tilde{z}_p(\theta_F)$ and $\tilde{z}_p'(\theta_F)$, as given in the above equation, so this equation can be thought of as representing the boundary conditions.

3.2. Solution to in-plane maneuvers

In-plane motion seems to be somewhat cumbersome because x and y are coupled. This is because relative motion is described in a noninertial frame. However, the analysis is parallel to the out-of-plane case. The relative equation for in-plane motion (Eq. (5a)) is

$$\boldsymbol{\Xi}' = \mathbf{A_{xy}}\boldsymbol{\Xi} + \mathbf{B_{xy}}\mathbf{U_{xy}}$$

This equation has the following solution:

$$\begin{bmatrix} \tilde{x}(\theta) \\ \tilde{x}'(\theta) \\ \tilde{y}(\theta) \\ \tilde{y}'(\theta) \end{bmatrix} = \boldsymbol{\Phi}_{\mathbf{xy}}(\theta)\boldsymbol{\Phi}_{\mathbf{xy}}^{-1}(\theta_0) \begin{bmatrix} \tilde{x}(\theta_0) \\ \tilde{x}'(\theta_0) \\ \tilde{y}(\theta_0) \\ \tilde{y}'(\theta_0) \end{bmatrix}$$

$$+\boldsymbol{\Phi}_{\mathbf{xy}}(\theta)\int_{\theta_0}^{\theta}\boldsymbol{\Phi}_{\mathbf{xy}}^{-1}(\tau)\begin{bmatrix}0&0\\1&0\\0&0\\0&1\end{bmatrix}\begin{bmatrix}u_x(\tau)\\u_y(\tau)\end{bmatrix}\mathrm{d}\tau \tag{12}$$

As in the out-of-plane case, the first term on the right is a homogeneous solution which enables the Deputy satellite to follow its own specific trajectory and the second is a particular solution with which the Deputy can be forced to arrive at the desired state. The fundamental matrix ($\boldsymbol{\Phi}_{\mathbf{xy}}$) associated with $\mathbf{A}_{\mathbf{xy}}$ is that given by Yamanaka and Ankersen [14]:

$$\boldsymbol{\Phi}_{\mathbf{xy}}(\theta)=\begin{bmatrix}0&-s&-c&3esK-2\\0&-s'&-c'&3e(s'K+s/\rho^2)\\1&-c(1+1/\rho)&s(1+1/\rho)&3\rho^2K\\0&2s&2c-e&3(1-2esK)\end{bmatrix} \tag{13a}$$

$$\boldsymbol{\Phi}_{\mathbf{xy}}^{-1}(\theta_0)=\frac{1}{1-e^2}\begin{bmatrix}-3e(s/\rho)(1+1/\rho)&ec-2&1-e^2&-es(1+1/\rho)\\3(s/\rho)(1+e^2/\rho)&2e-c&0&s(1+1/\rho)\\3(c/\rho+e)&s&0&c(1+1/\rho)+e\\1-e^2-3\rho&-es&0&-\rho^2\end{bmatrix}_{\theta=\theta_0} \tag{13b}$$

where $s=\rho\sin\theta$, $c=\rho\cos\theta$, $s'=\cos\theta+e\cos2\theta$, $c'=-(\sin\theta+e\sin2\theta)$, and

$$K(\theta)=\frac{1}{\Gamma^2}(t-t_0)=\int_{\theta_0}^{\theta}\frac{1}{\rho(\tau)^2}\,\mathrm{d}\tau \tag{14}$$

It is convenient to use $K(\theta)$ because it is directly obtained by observing the amount of time passed. Thus, the homogeneous solution to Eq. (5a) is

$$\begin{bmatrix}\hat{\tilde{x}}(\theta)\\\hat{\tilde{x}}'(\theta)\\\hat{\tilde{y}}(\theta)\\\hat{\tilde{y}}'(\theta)\end{bmatrix}=\boldsymbol{\Phi}_{\mathbf{xy}}(\theta)\boldsymbol{\Phi}_{\mathbf{xy}}^{-1}(\theta_0)\begin{bmatrix}\tilde{x}(\theta_0)\\\tilde{x}'(\theta_0)\\\tilde{y}(\theta_0)\\\tilde{y}'(\theta_0)\end{bmatrix} \tag{15a}$$

or

$$\begin{aligned}\begin{bmatrix}\hat{x}(\theta)\\\hat{\dot{x}}(\theta)\\\hat{y}(\theta)\\\hat{\dot{y}}(\theta)\end{bmatrix}&=\begin{bmatrix}\Gamma/\rho(\theta)&0&0&0\\e\sin\theta/\Gamma&\rho(\theta)/\Gamma&0&0\\0&0&\Gamma/\rho(\theta)&0\\0&0&e\sin\theta/\Gamma&\rho(\theta)/\Gamma\end{bmatrix}\\&\quad\times\boldsymbol{\Phi}_{\mathbf{xy}}(\theta)\boldsymbol{\Phi}_{\mathbf{xy}}^{-1}(\theta_0)\\&\quad\times\begin{bmatrix}\rho(\theta_0)/\Gamma&0&0&0\\-e\sin\theta_0/\Gamma&\Gamma/\rho(\theta_0)&0&0\\0&0&\rho(\theta_0)/\Gamma&0\\0&0&-e\sin\theta_0/\Gamma&\Gamma/\rho(\theta_0)\end{bmatrix}\\&\quad\times\begin{bmatrix}x(\theta_0)\\\dot{x}(\theta_0)\\y(\theta_0)\\\dot{y}(\theta_0)\end{bmatrix}\end{aligned} \tag{15b}$$

where the carat is again used to represent the state of the Deputy satellite if the thrust has not been applied.

Next, the particular solution to Eq. (5a) must be found, which requires the inverse of $\boldsymbol{\Phi}_{\mathbf{xy}}(\theta)$. Let $\boldsymbol{\Phi}_{\mathbf{xy}}^{-1}(\theta)$ take the following form:

$$\boldsymbol{\Phi}_{\mathbf{xy}}^{-1}(\theta)=\begin{bmatrix}P_{11}&P_{12}&P_{13}&P_{14}\\P_{21}&P_{22}&P_{23}&P_{24}\\P_{31}&P_{32}&P_{33}&P_{34}\\P_{41}&P_{42}&P_{43}&P_{44}\end{bmatrix}$$

where the components P_{ij} $(i,j=1,2,3,4)$ are given in Appendix A. If we define

$$\mathbf{Q}(\theta)\equiv\begin{bmatrix}Q_2(\theta)\\Q_3(\theta)\\Q_4(\theta)\\Q_5(\theta)\end{bmatrix}\equiv\int_{\theta_0}^{\theta}\boldsymbol{\Phi}_{\mathbf{xy}}^{-1}(\tau)\begin{bmatrix}0&0\\1&0\\0&0\\0&1\end{bmatrix}\begin{bmatrix}u_x(\tau)\\u_y(\tau)\end{bmatrix}\mathrm{d}\tau$$

then the particular solution will be

$$\begin{aligned}\begin{bmatrix}\tilde{x}_p(\theta)\\\tilde{x}_p'(\theta)\\\tilde{y}_p(\theta)\\\tilde{y}_p'(\theta)\end{bmatrix}&=\boldsymbol{\Phi}_{\mathbf{xy}}(\theta)\int_{\theta_0}^{\theta}\boldsymbol{\Phi}_{\mathbf{xy}}^{-1}(\tau)\begin{bmatrix}0&0\\1&0\\0&0\\0&1\end{bmatrix}\begin{bmatrix}u_x(\tau)\\u_y(\tau)\end{bmatrix}\mathrm{d}\tau\\&=\begin{bmatrix}0&-s&-c&3esK-2\\0&-s'&-c'&3e(s'K+s/\rho^2)\\1&-c(1+1/\rho)&s(1+1/\rho)&3\rho^2K\\0&2s&2c-e&3(1-2esK)\end{bmatrix}\\&\quad\times\begin{bmatrix}Q_2(\theta)\\Q_3(\theta)\\Q_4(\theta)\\Q_5(\theta)\end{bmatrix}\end{aligned} \tag{16}$$

where

$$\begin{bmatrix}Q_2(\theta)\\Q_3(\theta)\\Q_4(\theta)\\Q_5(\theta)\end{bmatrix}=\begin{bmatrix}S(P_{12}u_x)+S(P_{14}u_y)\\S(P_{22}u_x)+S(P_{24}u_y)\\S(P_{32}u_x)+S(P_{34}u_y)\\S(P_{42}u_x)+S(P_{44}u_y)\end{bmatrix}$$

and $S(\cdot)$ which means an integration is defined as

$$S(\cdot)=S\big[\cdot(\theta)\big]=\int_{\theta_0}^{\theta}\cdot(\tau)\,\mathrm{d}\tau$$

After thrust is applied during $\Delta\theta$, the satellite will reach a predefined state $[\tilde{x}(\theta_F),\tilde{x}'(\theta_F),\tilde{y}(\theta_F),\tilde{y}'(\theta_F)]^{\mathrm{T}}$. This places constraints on $u_x(\theta)$ and $u_y(\theta)$, creating the following relationships (from Eq. (16)):

$$\begin{bmatrix}Q_2(\theta_F)\\Q_3(\theta_F)\\Q_4(\theta_F)\\Q_5(\theta_F)\end{bmatrix}=\begin{bmatrix}P_{11}&P_{12}&P_{13}&P_{14}\\P_{21}&P_{22}&P_{23}&P_{24}\\P_{31}&P_{32}&P_{33}&P_{34}\\P_{41}&P_{42}&P_{43}&P_{44}\end{bmatrix}_{\theta=\theta_F}\begin{bmatrix}\tilde{x}_p(\theta_F)\\\tilde{x}_p'(\theta_F)\\\tilde{y}_p(\theta_F)\\\tilde{y}_p'(\theta_F)\end{bmatrix}$$

That is, we should find the $u_x(\theta)$ and $u_y(\theta)$ which satisfy the above equation at $\theta=\theta_F$. P_{ij} $(i,j=1,2,3,4)$ are given in Appendix A and the desired state $[\tilde{x}(\theta_F),\tilde{x}'(\theta_F),\tilde{y}(\theta_F),\tilde{y}'(\theta_F)]^{\mathrm{T}}$ is set at the actual desired position (x,y,z) and velocity $(\dot{x},\dot{y},\dot{z})$ using Eqs. (7a) and (7b).

In summary, when the Chief has θ $(\theta_0\leqslant\theta\leqslant\theta_F)$, the Deputy's position and velocity in the x–y plane will be

$$\begin{bmatrix}\tilde{x}(\theta)\\\tilde{x}'(\theta)\\\tilde{y}(\theta)\\\tilde{y}'(\theta)\end{bmatrix}=\begin{bmatrix}\hat{\tilde{x}}(\theta)\\\hat{\tilde{x}}'(\theta)\\\hat{\tilde{y}}(\theta)\\\hat{\tilde{y}}'(\theta)\end{bmatrix}+\begin{bmatrix}\tilde{x}_p(\theta)\\\tilde{x}_p'(\theta)\\\tilde{y}_p(\theta)\\\tilde{y}_p'(\theta)\end{bmatrix}$$

or

$$\begin{bmatrix} x(\theta) \\ \dot{x}(\theta) \\ y(\theta) \\ \dot{y}(\theta) \end{bmatrix} = \begin{bmatrix} \hat{x}(\theta) \\ \dot{\hat{x}}(\theta) \\ \hat{y}(\theta) \\ \dot{\hat{y}}(\theta) \end{bmatrix} + \begin{bmatrix} x_p(\theta) \\ \dot{x}_p(\theta) \\ y_p(\theta) \\ \dot{y}_p(\theta) \end{bmatrix}$$

The above equation could be rewritten as

$$\begin{aligned} &\begin{bmatrix} \tilde{x}(\theta) \\ \tilde{x}'(\theta) \\ \tilde{y}(\theta) \\ \tilde{y}'(\theta) \end{bmatrix} \\ &= \begin{bmatrix} \hat{\tilde{x}}(\theta) \\ \hat{\tilde{x}}'(\theta) \\ \hat{\tilde{y}}(\theta) \\ \hat{\tilde{y}}'(\theta) \end{bmatrix} \\ &\quad + \begin{bmatrix} 0 & -s & -c & 3esK-2 \\ 0 & -s' & -c' & 3e(s'K+s/\rho^2) \\ 1 & -c(1+1/\rho) & s(1+1/\rho) & 3\rho^2 K \\ 0 & 2s & 2c-e & 3(1-2esK) \end{bmatrix} \\ &\quad \times \begin{bmatrix} S(P_{12}u_x)+S(P_{14}u_y) \\ S(P_{22}u_x)+S(P_{24}u_y) \\ S(P_{32}u_x)+S(P_{34}u_y) \\ S(P_{42}u_x)+S(P_{44}u_y) \end{bmatrix} \end{aligned}$$

In the end, the Chief arrives at θ_F, then the x and y thrusters of the Deputy are turned off and the Deputy satisfies the constraints mentioned earlier:

$$\begin{aligned} \begin{bmatrix} Q_2(\theta_F) \\ Q_3(\theta_F) \\ Q_4(\theta_F) \\ Q_5(\theta_F) \end{bmatrix} &= \begin{bmatrix} S(P_{12}u_x)+S(P_{14}u_y) \\ S(P_{22}u_x)+S(P_{24}u_y) \\ S(P_{32}u_x)+S(P_{34}u_y) \\ S(P_{42}u_x)+S(P_{44}u_y) \end{bmatrix}_{\theta=\theta_F} \\ &= \begin{bmatrix} P_{11} & P_{12} & P_{13} & P_{14} \\ P_{21} & P_{22} & P_{23} & P_{24} \\ P_{31} & P_{32} & P_{33} & P_{34} \\ P_{41} & P_{42} & P_{43} & P_{44} \end{bmatrix}_{\theta=\theta_F} \begin{bmatrix} \tilde{x}_p(\theta_F) \\ \tilde{x}'_p(\theta_F) \\ \tilde{y}_p(\theta_F) \\ \tilde{y}'_p(\theta_F) \end{bmatrix} \\ &= \begin{bmatrix} P_{11} & P_{12} & P_{13} & P_{14} \\ P_{21} & P_{22} & P_{23} & P_{24} \\ P_{31} & P_{32} & P_{33} & P_{34} \\ P_{41} & P_{42} & P_{43} & P_{44} \end{bmatrix}_{\theta=\theta_F} \begin{bmatrix} \tilde{x}(\theta_F)-\hat{\tilde{x}}(\theta_F) \\ \tilde{x}'(\theta_F)-\hat{\tilde{x}}'(\theta_F) \\ \tilde{y}(\theta_F)-\hat{\tilde{y}}(\theta_F) \\ \tilde{y}'(\theta_F)-\hat{\tilde{y}}'(\theta_F) \end{bmatrix} \end{aligned}$$

Of course, the states above have pseudo-values, so they must be evaluated from the actual values by Eqs. (7a) and (7b).

4. Thrust accelerations in a Fourier series

Our objective is to relocate the Deputy to the desired position relative to the Chief while minimizing fuel consumption. In general, the following performance index is used for fuel-optimality

$$\begin{aligned} J &= \int_{t_0}^{t_F} \mathbf{T}^{\mathrm{T}}\mathbf{R}\mathbf{T}\,\mathrm{d}t \\ &= \int_{\theta_0}^{\theta_F} \mathbf{T}^{\mathrm{T}}\mathbf{R}\mathbf{T}\frac{dt}{d\theta}\,\mathrm{d}\theta \\ &= \Gamma^2 \int_{\theta_0}^{\theta_F} \frac{\mathbf{T}^{\mathrm{T}}\mathbf{R}\mathbf{T}}{\rho^2(\theta)}\,\mathrm{d}\theta \end{aligned} \tag{17}$$

where $\mathbf{T} = [T_x\ T_y\ T_z]^{\mathrm{T}}$ is a thrust acceleration vector of the Deputy and the matrix $\mathbf{R}$ is a 3 by 3 weight matrix. In this paper, however, the following performance index is employed:

$$J = \int_{\theta_0}^{\theta_F} \mathbf{T}^{\mathrm{T}}(\tau)\mathbf{T}(\tau)\,\mathrm{d}\tau = \int_{\theta_0}^{\theta_F} T(\tau)^2\,\mathrm{d}\tau \tag{18}$$

where τ is used as an integration variable, $T(\tau)^2 = T_x(\tau)^2 + T_y(\tau)^2 + T_z(\tau)^2$, and the low levels of thrusters are operated for the Chief satellite's $\theta_0 \leqslant \theta \leqslant \theta_F$. Although the control law developed from Eq. (18) is not strictly fuel-optimal and the effect of the denominator $\rho^2(\theta)$ in Eq. (17) is not negligible for moderate or high eccentricities, setting a performance index as Eq. (18) enables a complete analytical approach as will be seen. Also, the effect of $\rho(\theta)$ can be mitigated by choosing an appropriate gain matrix $\mathbf{R}$ and the use of Eq. (18) naturally penalizes the control effort near perigee [10,9]. Because the out-of-plane motion is decoupled from the in-plane motion, we can define the next two performance indices from Eq. (18):

$$J_z = \int_{\theta_0}^{\theta_F} T_z(\tau)^2\,\mathrm{d}\tau \tag{19a}$$

and

$$J_{xy} = \int_{\theta_0}^{\theta_F} \left[T_x(\tau)^2 + T_y(\tau)^2\right]\mathrm{d}\tau \tag{19b}$$

We must also incorporate the constraints formulated in the previous section and find the thrust functions in terms of the true anomaly. The question is how we can represent general thrust functions. Using a Fourier series can yield an appropriate answer. While thrust functions may be discontinuous or impossible to differentiate, generating a description of thrust function by a Fourier series can solve this troublesome problem. Since it satisfies Dirichlet conditions, that is, it has a finite number of finite discontinuities and has a finite number of extrema, any thrust function can be mathematically represented in a Fourier series that converges to the function at continuous points and the mean of the positive and negative limits at points of discontinuity. In brief, we can think of each thrust function as a Fourier series with the period $\Delta\theta = \theta_F - \theta_0$. Then, the thrust acceleration in a Fourier series with domain $\theta_0 \leqslant \theta \leqslant \theta_F$ can be obtained. Therefore, the performance indices can be represented by Fourier coefficients that satisfy the preceding constraints.

Thrust functions in a Fourier series are obtained as follows:

$$T_x(\theta) = \frac{a_{x0}}{2} + \sum_{n=1}^{\infty}\left(a_{xn}\cos\frac{2n\pi}{\Delta\theta}\theta + b_{xn}\sin\frac{2n\pi}{\Delta\theta}\theta\right) \tag{20a}$$

$$T_y(\theta) = \frac{a_{y0}}{2} + \sum_{n=1}^{\infty}\left(a_{yn}\cos\frac{2n\pi}{\Delta\theta}\theta + b_{yn}\sin\frac{2n\pi}{\Delta\theta}\theta\right) \tag{20b}$$

$$T_z(\theta) = \frac{a_{z0}}{2} + \sum_{n=1}^{\infty}\left(a_{zn}\cos\frac{2n\pi}{\Delta\theta}\theta + b_{zn}\sin\frac{2n\pi}{\Delta\theta}\theta\right) \tag{20c}$$

where

$$a_{x0} = \frac{2}{\Delta\theta}\int_{\theta_0}^{\theta_F} T_x(\theta)\,\mathrm{d}\theta, \qquad a_{xn} = \frac{2}{\Delta\theta}\int_{\theta_0}^{\theta_F} T_x(\theta)\cos\frac{2n\pi}{\Delta\theta}\theta\,\mathrm{d}\theta$$

$$b_{xn} = \frac{2}{\Delta\theta}\int_{\theta_0}^{\theta_F} T_x(\theta)\sin\frac{2n\pi}{\Delta\theta}\theta\,\mathrm{d}\theta$$

$$a_{y0} = \frac{2}{\Delta\theta}\int_{\theta_0}^{\theta_F} T_y(\theta)\,\mathrm{d}\theta, \qquad a_{yn} = \frac{2}{\Delta\theta}\int_{\theta_0}^{\theta_F} T_y(\theta)\cos\frac{2n\pi}{\Delta\theta}\theta\,\mathrm{d}\theta$$

$$b_{yn} = \frac{2}{\Delta\theta}\int_{\theta_0}^{\theta_F} T_y(\theta)\sin\frac{2n\pi}{\Delta\theta}\theta\,\mathrm{d}\theta$$

$$a_{z0} = \frac{2}{\Delta\theta}\int_{\theta_0}^{\theta_F} T_z(\theta)\,\mathrm{d}\theta, \qquad a_{zn} = \frac{2}{\Delta\theta}\int_{\theta_0}^{\theta_F} T_z(\theta)\cos\frac{2n\pi}{\Delta\theta}\theta\,\mathrm{d}\theta$$

$$b_{zn} = \frac{2}{\Delta\theta}\int_{\theta_0}^{\theta_F} T_z(\theta)\sin\frac{2n\pi}{\Delta\theta}\theta\,\mathrm{d}\theta$$

If Parseval's theorem [2], which represents the relationship between the average of the square of $T(\theta)$ and the Fourier coefficients, is used, the performance index for the z thrust function can be written as

$$J_z = \frac{\Delta\theta}{2}\left[\frac{a_{z0}^2}{2} + \sum_{n=1}^{\infty}\left(a_{zn}^2 + b_{zn}^2\right)\right] \tag{21a}$$

and the performance index for the coupled x and y thrust accelerations is

$$J_{xy} = \frac{\Delta\theta}{2}\left[\frac{a_{x0}^2}{2} + \sum_{n=1}^{\infty}\left(a_{xn}^2 + b_{xn}^2\right)\right] + \frac{\Delta\theta}{2}\left[\frac{a_{y0}^2}{2} + \sum_{n=1}^{\infty}\left(a_{yn}^2 + b_{yn}^2\right)\right] \tag{21b}$$

Now, we must find those Fourier coefficients $(a_{x0}, a_{xn}, b_{xn}, a_{y0}, a_{yn}, b_{yn})$ which minimize the performance indices J_{xy} and J_z. In doing so, we must not forget to incorporate boundary constraints. For this, it is best to represent the boundary constraints in terms of Fourier coefficients. We find those coefficients which yield the optimal thrust accelerations by minimizing the performance indices with respect to the coefficients. Let us consider the out-of-plane case first, and then the in-plane case.

4.1. Out-of-plane thrust functions

For the out-of-plane thrust function, there exist constraints on $\tilde{z}(\theta_F)$ and $\tilde{z}'(\theta_F)$ because we wish to set the Deputy to a desired state. The particular solutions which indicate the thrust necessary to put the Deputy into the desired state can be thought of as boundary conditions. Here, rather than the original constraints, $\tilde{z}(\theta_F)$ and $\tilde{z}'(\theta_F)$, new transformed constraints I_0 and I_1 are introduced for a simpler calculation. This is just a coordinate transformation:

$$\begin{bmatrix} I_0 \\ I_1 \end{bmatrix} = \begin{bmatrix} \sin\theta_F & \cos\theta_F \\ -\cos\theta_F & \sin\theta_F \end{bmatrix}\begin{bmatrix} \tilde{z}_p(\theta_F) \\ \tilde{z}'_p(\theta_F) \end{bmatrix} = \begin{bmatrix} \Gamma^3\int_{\theta_0}^{\theta_F}\frac{\cos\tau}{\rho(\tau)^3}T_z(\tau)\,\mathrm{d}\tau \\ \Gamma^3\int_{\theta_0}^{\theta_F}\frac{\sin\tau}{\rho(\tau)^3}T_z(\tau)\,\mathrm{d}\tau \end{bmatrix} \tag{22}$$

Substituting Eq. (20c) into Eq. (22), we obtain

$$I_0 = \frac{f_{z0}a_{z0}}{2} + \sum_{n=1}^{\infty} f_{za}(n)a_{zn} + \sum_{n=1}^{\infty} f_{zb}(n)b_{zn} \tag{23a}$$

$$I_1 = \frac{g_{z0}a_{z0}}{2} + \sum_{n=1}^{\infty} g_{za}(n)a_{zn} + \sum_{n=1}^{\infty} g_{zb}(n)b_{zn} \tag{23b}$$

where

$$f_{z0} = \Gamma^3\int_{\theta_0}^{\theta_F}\frac{\cos\tau}{(1+e\cos\tau)^3}\,\mathrm{d}\tau$$

$$f_{za}(n) = \Gamma^3\int_{\theta_0}^{\theta_F}\frac{\cos\tau}{(1+e\cos\tau)^3}\cos\frac{2n\pi}{\Delta\theta}\tau\,\mathrm{d}\tau$$

$$f_{zb}(n) = \Gamma^3\int_{\theta_0}^{\theta_F}\frac{\cos\tau}{(1+e\cos\tau)^3}\sin\frac{2n\pi}{\Delta\theta}\tau\,\mathrm{d}\tau \tag{24a}$$

$$g_{z0} = \Gamma^3\int_{\theta_0}^{\theta_F}\frac{\sin\tau}{(1+e\cos\tau)^3}\,\mathrm{d}\tau$$

$$g_{za}(n) = \Gamma^3\int_{\theta_0}^{\theta_F}\frac{\sin\tau}{(1+e\cos\tau)^3}\cos\frac{2n\pi}{\Delta\theta}\tau\,\mathrm{d}\tau$$

$$g_{zb}(n) = \Gamma^3\int_{\theta_0}^{\theta_F}\frac{\sin\tau}{(1+e\cos\tau)^3}\sin\frac{2n\pi}{\Delta\theta}\tau\,\mathrm{d}\tau \tag{24b}$$

where $\Delta\theta = \theta_F - \theta_0$. It is noted that Eqs. (23a) and (23b) represent the constraints in terms of Fourier coefficients. Incorporating the constraints (Eqs. (23a) and (23b)) using Lagrange multipliers λ_0 and λ_1, the augmented performance index $J_{z,aug}$ obtains the following:

$$J_{z,aug} = \frac{\Delta\theta}{2}\left[\frac{a_{z0}^2}{2} + \sum_{n=1}^{\infty}a_{zn}^2 + \sum_{n=1}^{\infty}b_{zn}^2\right] + \lambda_0\left[I_0 - \frac{f_{z0}a_{z0}}{2} - \sum_{n=1}^{\infty}f_{za}(n)a_{zn} - \sum_{n=1}^{\infty}f_{zb}(n)b_{zn}\right] + \lambda_1\left[I_1 - \frac{g_{z0}a_{z0}}{2} - \sum_{n=1}^{\infty}g_{za}(n)a_{zn} - \sum_{n=1}^{\infty}g_{zb}(n)b_{zn}\right] \tag{25}$$

Then, partially differentiating Eq. (25) with respect to the respective Fourier coefficients a_{z0}, a_{zn}, b_{zn}, and setting the results equal to zero, the coefficients for the optimal maneuver are obtained as follows to minimize the performance index:

$$a_{z0} = \frac{1}{\Delta\theta}[\lambda_0 f_{z0} + \lambda_1 g_{z0}]$$

$$a_{zn}(n) = \frac{1}{\Delta\theta}\left[\lambda_0 f_{zn}(n) + \lambda_1 g_{zn}(n)\right]$$

$$b_{zn}(n) = \frac{1}{\Delta\theta}\left[\lambda_0 f_{zb}(n) + \lambda_1 g_{zb}(n)\right] \tag{26}$$

Substituting Eq. (26) into Eqs. (23a) and (23b), I_0 and I_1 are rewritten in terms of λ_0 and λ_1:

$$\begin{bmatrix} I_0 \\ I_1 \end{bmatrix} = \begin{bmatrix} p_0 & p_1 \\ p_1 & q_1 \end{bmatrix}\begin{bmatrix} \lambda_0 \\ \lambda_1 \end{bmatrix} \tag{27}$$

where

$$p_0 = \frac{f_{z0}^2}{2\Delta\theta} + \frac{1}{\Delta\theta}\sum_{n=1}^{\infty}\left[f_{za}(n)^2 + f_{zb}(n)^2\right]$$

$$p_1 = \frac{f_{z0}g_{z0}}{2\Delta\theta} + \frac{1}{\Delta\theta}\sum_{n=1}^{\infty}\left[f_{za}(n)g_{za}(n) + f_{zb}(n)g_{zb}(n)\right]$$

$$q_1 = \frac{g_{z0}^2}{2\Delta\theta} + \frac{1}{\Delta\theta}\sum_{n=1}^{\infty}\left[g_{za}(n)^2 + g_{zb}(n)^2\right]$$

p_0, p_1, and q_1 contain the infinite series. However, by Parseval's theorem, all of these infinite sums converge at constant values:

$$\begin{aligned}
p_0 &= \frac{\Gamma^6}{2}\int_{\theta_0}^{\theta_F}\frac{\cos^2\tau}{(1+e\cos\tau)^6}\,\mathrm{d}\tau \\
&= \frac{\Gamma^6}{2(1-e^2)^{11/2}}\Big[-\frac{1}{80}e^3\sin 5E + \frac{1}{32}e^2(2e^2+3)\sin 4E \\
&\quad - \frac{1}{8}e\big(6e^4+65e^2+34\big)\sin E \\
&\quad - \frac{1}{48}e\big(4e^4+29e^2+12\big)\sin 3E \\
&\quad + \frac{1}{8}\big(18e^4+41e^2+4\big)E + \frac{1}{4}\big(5e^4+9e^2+1\big)\sin 2E\Big]_{E_0}^{E_F} \\
p_1 &= \frac{\Gamma^6}{2}\int_{\theta_0}^{\theta_F}\frac{\cos\tau\sin\tau}{(1+e\cos\tau)^6}\,\mathrm{d}\tau \\
&= \frac{\Gamma^6}{2(1-e^2)^5}\Big[\frac{1}{80}e^3\cos 5E - \frac{1}{32}\big(e^2+3\big)e^2\cos 4E \\
&\quad + \frac{7}{8}e\big(e^2+2\big)\cos E + \frac{1}{16}e\big(5e^2+4\big)\cos 3E \\
&\quad - \frac{1}{8}\big(e^4+9e^2+2\big)\cos 2E\Big]_{E_0}^{E_F} \\
q_1 &= \frac{\Gamma^6}{2}\int_{\theta_0}^{\theta_F}\frac{\sin^2\tau}{(1+e\cos\tau)^6}\,\mathrm{d}\tau \\
&= \frac{\Gamma^6}{2(1-e^2)^{9/2}}\Big[\frac{1}{80}e^3\sin 5E - \frac{3}{32}e^2\sin 4E - \frac{1}{8}e\big(e^2+6\big)\sin E \\
&\quad + \frac{1}{48}e\big(e^2+12\big)\sin 3E + \frac{1}{8}\big(3e^2+4\big)E - \frac{1}{4}\sin 2E\Big]_{E_0}^{E_F}
\end{aligned}$$

where E is the eccentric anomaly corresponding to the true anomaly θ, and the followings hold true [13]:

$$\cos\theta = \frac{\cos E - e}{1-e\cos E}, \qquad \sin\theta = \frac{\sin E\sqrt{1-e^2}}{1-e\cos E}$$

$$\tan\frac{\theta}{2} = \sqrt{\frac{1+e}{1-e}}\tan\frac{E}{2}$$

The last identity is very convenient because it alleviates the quadrant ambiguity. From Eq. (27), we have convenient closed-form parameters to represent the Lagrange multipliers λ_0 and λ_1:

$$\begin{bmatrix}\lambda_0\\ \lambda_1\end{bmatrix} = \frac{1}{p_0q_1 - p_1^2}\begin{bmatrix}q_1 & -p_1\\ -p_1 & p_0\end{bmatrix}\begin{bmatrix}I_0\\ I_1\end{bmatrix} \tag{28}$$

It is noted that p_0, p_1, q_1, I_0, and I_1 are all constants. Finally, we use these parameters to express the optimal thrust acceleration $T_z(\theta)$, producing:

$$\begin{aligned}
T_z(\theta) &= \frac{a_{z0}}{2} + \sum_{n=1}^{\infty}a_{zn}\cos\left(\frac{2n\pi}{\Delta\theta}\theta\right) + \sum_{n=1}^{\infty}b_{zn}\sin\left(\frac{2n\pi}{\Delta\theta}\theta\right) \\
&= \frac{1}{2\Delta\theta}(\lambda_0 f_{z0} + \lambda_1 g_{z0}) \\
&\quad + \frac{1}{\Delta\theta}\sum_{n=1}^{\infty}\left[\lambda_0 f_{za}(n) + \lambda_1 g_{za}(n)\right]\cos\left(\frac{2n\pi}{\Delta\theta}\theta\right) \\
&\quad + \frac{1}{\Delta\theta}\sum_{n=1}^{\infty}\left[\lambda_0 f_{zb}(n) + \lambda_1 g_{zb}(n)\right]\sin\left(\frac{2n\pi}{\Delta\theta}\theta\right)
\end{aligned} \tag{29}$$

Eq. (29) can be simplified into the following closed-form solution by Parseval's theorem:

$$T_z(\theta) = \frac{\Gamma^3}{2}\left[\frac{\lambda_0\cos\theta + \lambda_1\sin\theta}{(1+e\cos\theta)^3}\right] \tag{30}$$

Eq. (30) is the final result for $T_z(\theta)$ which is a z-component of thrust for the optimal reconfiguration of satellites in an elliptic orbit. Furthermore, it is not difficult to show that Eq. (30) replicates Palmer's result (Eq. (30) in [8]) when $e = 0$. (See Appendix C.) We use Eq. (28) to evaluate λ_0 and λ_1 in which I_0 and I_1 are determined from Eq. (22). The performance index Eq. (21a) is then represented in a simple closed form as follows:

$$J_z = \frac{1}{2}(I_0\lambda_0 + I_1\lambda_1) \tag{31}$$

In addition, if Eq. (30) is inserted into Eqs. (11a) and (11b), we can obtain the variations in z and $\dot{z}$:

$$\begin{aligned}
\tilde{z}_p(\theta) &= \frac{\Gamma^6}{2}\big[\lambda_0\big(\sin\theta A_1(\theta) - \cos\theta A_2(\theta)\big) \\
&\quad + \lambda_1\big(\sin\theta A_2(\theta) - \cos\theta A_3(\theta)\big)\big] \\
\tilde{z}'_p(\theta) &= \frac{\Gamma^6}{2}\big[\lambda_0\big(\cos\theta A_1(\theta) + \sin\theta A_2(\theta)\big) \\
&\quad + \lambda_1\big(\cos\theta A_2(\theta) + \sin\theta A_3(\theta)\big)\big]
\end{aligned} \tag{32}$$

where

$$A_1(\theta) = S\left[\frac{\cos^2\theta}{\rho(\theta)^6}\right] = \int_{\theta_0}^{\theta}\frac{\cos^2\tau}{(1+e\cos\tau)^6}\,\mathrm{d}\tau$$

$$A_2(\theta) = S\left[\frac{\cos\theta\sin\theta}{\rho(\theta)^6}\right] = \int_{\theta_0}^{\theta}\frac{\cos\tau\sin\tau}{(1+e\cos\tau)^6}\,\mathrm{d}\tau$$

and

$$A_3(\theta) = S\left[\frac{\sin^2\theta}{\rho(\theta)^6}\right] = \int_{\theta_0}^{\theta}\frac{\sin^2\tau}{(1+e\cos\tau)^6}\,\mathrm{d}\tau$$

are given in Appendix B. From Eqs. (6a) and (6b), the actual position and velocity for the z-component are, respectively,

$$\begin{aligned}
z_p(\theta) &= \frac{\Gamma^7}{2\rho(\theta)}\big[\lambda_0\big(\sin\theta A_1(\theta) - \cos\theta A_2(\theta)\big) \\
&\quad + \lambda_1\big(\sin\theta A_2(\theta) - \cos\theta A_3(\theta)\big)\big] \\
\dot{z}_p(\theta) &= \frac{\Gamma^5}{2}\big[\lambda_0\big((e+\cos\theta)A_1(\theta) + \sin\theta A_2(\theta)\big) \\
&\quad + \lambda_1\big((e+\cos\theta)A_2(\theta) + \sin\theta A_3(\theta)\big)\big]
\end{aligned} \tag{33}$$

If $z_p(\theta)$ and $\dot{z}_p(\theta)$ are found, we then know the z-component of the Deputy's position and velocity during the maneuver by adding the homogeneous solutions of Eq. (10b).

4.2. In-plane thrust functions

In the coupled case for in-plane motion, the equations are more complicated while the process is similar to that for out-of-plane motion, as described in the previous section. First the constraints for the Deputy satellite at a desired $\theta = \theta_F$ should be evaluated. In doing so, we consider the transformed constraints I_2, I_3, I_4, I_5 instead of the existing constraints $[Q_2(\theta_F), Q_3(\theta_F), Q_4(\theta_F), Q_5(\theta_F)]^{\mathrm{T}}$:

$$\begin{bmatrix} I_2 \\ I_3 \\ I_4 \\ I_5 \end{bmatrix} = \begin{bmatrix} e & 1 & 0 & 0 \\ 1 & e & 0 & 0 \\ 0 & 0 & e & 1 \\ 0 & 0 & 1 & e \end{bmatrix} \begin{bmatrix} Q_2(\theta_F) \\ Q_3(\theta_F) \\ Q_4(\theta_F) \\ Q_5(\theta_F) \end{bmatrix} = \begin{bmatrix} -\Gamma^3 \int_{\theta_0}^{\theta_F} \frac{T_x(\tau)}{\rho(\tau)^2} \cos\tau \,\mathrm{d}\tau + \Gamma^3 \int_{\theta_0}^{\theta_F} \frac{T_y(\tau)}{\rho(\tau)^3} (1+\rho(\tau)) \sin\tau \,\mathrm{d}\tau \\ \Gamma^3 \int_{\theta_0}^{\theta_F} \frac{T_x(\tau)}{\rho(\tau)^3} (3e\sin\tau\rho(\tau)K(\tau) - 2) \,\mathrm{d}\tau + 3\Gamma^3 \int_{\theta_0}^{\theta_F} \frac{T_y(\tau)}{\rho(\tau)} K(\tau) \,\mathrm{d}\tau \\ -\Gamma^3 \int_{\theta_0}^{\theta_F} \frac{T_y(\tau)}{\rho(\tau)^3} \,\mathrm{d}\tau \\ \Gamma^3 \int_{\theta_0}^{\theta_F} \frac{T_x(\tau)}{\rho(\tau)^2} \sin\tau \,\mathrm{d}\tau + \Gamma^3 \int_{\theta_0}^{\theta_F} \frac{T_y(\tau)}{\rho(\tau)^3} (1+\rho(\tau)) \cos\tau \,\mathrm{d}\tau \end{bmatrix} \tag{34}$$

The cue for these new constraints is taken from the $\boldsymbol{\Phi}_{\mathbf{xy}}^{-1}(\theta)$ form (see Appendix A). For example, P_{12} and P_{22} are related by $\left[\begin{smallmatrix} P_{12} \\ P_{22} \end{smallmatrix}\right] = \frac{1}{D}\left[\begin{smallmatrix} e & 1 \\ 1 & e \end{smallmatrix}\right]\left[\begin{smallmatrix} \phi_{12} \\ \phi_{22} \end{smallmatrix}\right]$, where $D = e^2 - 1$, $\phi_{12} = -\cos\theta\rho(\theta)$, and $\phi_{22} = 3e\sin\theta\rho(\theta)K(\theta) - 2$. Inserting Eqs. (20a) and (20b) into Eq. (34) gives

$$\begin{aligned} I_2 &= \frac{1}{2}h_{x0}a_{x0} + \sum_{n=1}^{\infty} h_{xa}(n)a_{xn} + \sum_{n=1}^{\infty} h_{xb}(n)b_{xn} + \frac{1}{2}j_{y0}a_{y0} \\ &\quad + \sum_{n=1}^{\infty} j_{ya}(n)a_{yn} + \sum_{n=1}^{\infty} j_{yb}(n)b_{yn} \\ I_3 &= \frac{1}{2}k_{x0}a_{x0} + \sum_{n=1}^{\infty} k_{xa}(n)a_{xn} + \sum_{n=1}^{\infty} k_{xb}(n)b_{xn} + \frac{1}{2}l_{y0}a_{y0} \\ &\quad + \sum_{n=1}^{\infty} l_{ya}(n)a_{yn} + \sum_{n=1}^{\infty} l_{yb}(n)b_{yn} \\ I_4 &= \frac{1}{2}m_{y0}a_{y0} + \sum_{n=1}^{\infty} m_{ya}(n)a_{yn} + \sum_{n=1}^{\infty} m_{yb}(n)b_{yn} \\ I_5 &= \frac{1}{2}n_{x0}a_{x0} + \sum_{n=1}^{\infty} n_{xa}(n)a_{xn} + \sum_{n=1}^{\infty} n_{xb}(n)b_{xn} + \frac{1}{2}p_{y0}a_{y0} \\ &\quad + \sum_{n=1}^{\infty} p_{ya}(n)a_{yn} + \sum_{n=1}^{\infty} p_{yb}(n)b_{yn} \end{aligned} \tag{35}$$

where

$$h_{x0} = -\Gamma^3 \int_{\theta_0}^{\theta_F} \frac{\cos\tau}{\rho^2} \,\mathrm{d}\tau, \qquad h_{xa}(n) = -\Gamma^3 \int_{\theta_0}^{\theta_F} \frac{\cos\tau}{\rho^2} \cos\frac{2n\pi}{\Delta\theta}\tau \,\mathrm{d}\tau$$

$$h_{xb}(n) = -\Gamma^3 \int_{\theta_0}^{\theta_F} \frac{\cos\tau}{\rho^2} \sin\frac{2n\pi}{\Delta\theta}\tau \,\mathrm{d}\tau$$

$$j_{y0} = \Gamma^3 \int_{\theta_0}^{\theta_F} \frac{1+\rho}{\rho^3} \sin\tau \,\mathrm{d}\tau$$

$$j_{ya}(n) = \Gamma^3 \int_{\theta_0}^{\theta_F} \frac{1+\rho}{\rho^3} \sin\tau \cos\frac{2n\pi}{\Delta\theta}\tau \,\mathrm{d}\tau$$

$$j_{yb}(n) = \Gamma^3 \int_{\theta_0}^{\theta_F} \frac{1+\rho}{\rho^3} \sin\tau \sin\frac{2n\pi}{\Delta\theta}\tau \,\mathrm{d}\tau$$

$$k_{x0} = \Gamma^3 \int_{\theta_0}^{\theta_F} \frac{3e\rho K\sin\tau - 2}{\rho^3} \,\mathrm{d}\tau$$

$$k_{xa}(n) = \Gamma^3 \int_{\theta_0}^{\theta_F} \frac{3e\rho K\sin\tau - 2}{\rho^3} \cos\frac{2n\pi}{\Delta\theta}\tau \,\mathrm{d}\tau$$

$$k_{xb}(n) = \Gamma^3 \int_{\theta_0}^{\theta_F} \frac{3e\rho K\sin\tau - 2}{\rho^3} \sin\frac{2n\pi}{\Delta\theta}\tau \,\mathrm{d}\tau$$

$$l_{y0} = 3\Gamma^3 \int_{\theta_0}^{\theta_F} \frac{K}{\rho} \,\mathrm{d}\tau, \qquad l_{ya}(n) = 3\Gamma^3 \int_{\theta_0}^{\theta_F} \frac{K}{\rho} \cos\frac{2n\pi}{\Delta\theta}\tau \,\mathrm{d}\tau$$

$$l_{yb}(n) = 3\Gamma^3 \int_{\theta_0}^{\theta_F} \frac{K}{\rho} \sin\frac{2n\pi}{\Delta\theta}\tau \,\mathrm{d}\tau$$

$$m_{y0} = -\Gamma^3 \int_{\theta_0}^{\theta_F} \frac{1}{\rho^3} \,\mathrm{d}\tau, \qquad m_{ya}(n) = -\Gamma^3 \int_{\theta_0}^{\theta_F} \frac{1}{\rho^3} \cos\frac{2n\pi}{\Delta\theta}\tau \,\mathrm{d}\tau$$

$$m_{yb}(n) = -\Gamma^3 \int_{\theta_0}^{\theta_F} \frac{1}{\rho^3} \sin\frac{2n\pi}{\Delta\theta}\tau \,\mathrm{d}\tau$$

$$n_{x0} = \Gamma^3 \int_{\theta_0}^{\theta_F} \frac{\sin\tau}{\rho^2} \,\mathrm{d}\tau, \qquad n_{xa}(n) = \Gamma^3 \int_{\theta_0}^{\theta_F} \frac{\sin\tau}{\rho^2} \cos\frac{2n\pi}{\Delta\theta}\tau \,\mathrm{d}\tau$$

$$n_{xb}(n) = \Gamma^3 \int_{\theta_0}^{\theta_F} \frac{\sin\tau}{\rho^2} \sin\frac{2n\pi}{\Delta\theta}\tau \,\mathrm{d}\tau$$

$$p_{y0} = \Gamma^3 \int_{\theta_0}^{\theta_F} \frac{1+\rho}{\rho^3} \cos\tau \,\mathrm{d}\tau$$

$$p_{ya}(n) = \Gamma^3 \int_{\theta_0}^{\theta_F} \frac{1+\rho}{\rho^3} \cos\tau \cos\frac{2n\pi}{\Delta\theta}\tau \,\mathrm{d}\tau$$

$$p_{yb}(n) = \Gamma^3 \int_{\theta_0}^{\theta_F} \frac{1+\rho}{\rho^3} \cos\tau \sin\frac{2n\pi}{\Delta\theta}\tau \,\mathrm{d}\tau \tag{36}$$

With Eq. (35) the constraints are thought of as the functions of the Fourier coefficients. Next, we must incorporate the constraints of Eq. (35) using constant Lagrange multipliers $(\lambda_2, \lambda_3, \lambda_4, \lambda_5)$ to get an augmented performance index $J_{xy,aug}$. We obtain the following:

$$\begin{aligned} J_{xy,aug} &= \frac{\Delta\theta}{2}\left[\frac{a_{x0}^2}{2} + \sum_{n=1}^{\infty} a_{xn}^2 + \sum_{n=1}^{\infty} b_{xn}^2\right] \\ &\quad + \frac{\Delta\theta}{2}\left[\frac{a_{y0}^2}{2} + \sum_{n=1}^{\infty} a_{yn}^2 + \sum_{n=1}^{\infty} b_{yn}^2\right] \end{aligned}$$

$$
\begin{aligned}
&+\lambda_2\Bigg[I_2-\frac{1}{2}h_{x0}a_{x0}-\sum_{n=1}^{\infty}h_{xa}(n)a_{xn}-\sum_{n=1}^{\infty}h_{xb}(n)b_{xn}\\
&-\frac{1}{2}j_{y0}a_{y0}-\sum_{n=1}^{\infty}j_{ya}(n)a_{yn}-\sum_{n=1}^{\infty}j_{yb}(n)b_{yn}\Bigg]\\
&+\lambda_3\Bigg[I_3-\frac{1}{2}k_{x0}a_{x0}-\sum_{n=1}^{\infty}k_{xa}(n)a_{xn}-\sum_{n=1}^{\infty}k_{xb}(n)b_{xn}\\
&-\frac{1}{2}l_{y0}a_{y0}-\sum_{n=1}^{\infty}l_{ya}(n)a_{yn}-\sum_{n=1}^{\infty}l_{yb}(n)b_{yn}\Bigg]\\
&+\lambda_4\Bigg[I_4-\frac{1}{2}m_{y0}a_{y0}-\sum_{n=1}^{\infty}m_{ya}(n)a_{yn}\\
&-\sum_{n=1}^{\infty}m_{yb}(n)b_{yn}\Bigg]\\
&+\lambda_5\Bigg[I_5-\frac{1}{2}n_{x0}a_{x0}-\sum_{n=1}^{\infty}n_{xa}(n)a_{xn}-\sum_{n=1}^{\infty}n_{xb}(n)b_{xn}\\
&-\frac{1}{2}p_{y0}a_{y0}-\sum_{n=1}^{\infty}p_{ya}(n)a_{yn}-\sum_{n=1}^{\infty}p_{yb}(n)b_{yn}\Bigg] \qquad (37)
\end{aligned}
$$

After partially differentiating Eq. (37) with respect to the associated Fourier coefficients and setting the results equal to zero to minimize the performance index, we get

$$
\begin{aligned}
a_{x0}&=\frac{1}{\Delta\theta}(\lambda_2h_{x0}+\lambda_3k_{x0}+\lambda_5n_{x0})\\
a_{xn}&=\frac{1}{\Delta\theta}(\lambda_2h_{xa}+\lambda_3k_{xa}+\lambda_5n_{xa})\\
b_{xn}&=\frac{1}{\Delta\theta}(\lambda_2h_{xb}+\lambda_3k_{xb}+\lambda_5n_{xb})\\
a_{y0}&=\frac{1}{\Delta\theta}(\lambda_2j_{y0}+\lambda_3l_{y0}+\lambda_4m_{y0}+\lambda_5p_{y0})\\
a_{yn}&=\frac{1}{\Delta\theta}(\lambda_2j_{ya}+\lambda_3l_{ya}+\lambda_4m_{ya}+\lambda_5p_{ya})\\
b_{y0}&=\frac{1}{\Delta\theta}(\lambda_2j_{yb}+\lambda_3l_{yb}+\lambda_4m_{yb}+\lambda_5p_{yb}) \qquad (38)
\end{aligned}
$$

If we substitute Eq. (38) into Eq. (35), the results from I_2 to I_5 become as follows:

$$
\begin{bmatrix}I_2\\I_3\\I_4\\I_5\end{bmatrix}=\begin{bmatrix}p_2&p_3&p_4&p_5\\p_3&q_3&q_4&q_5\\p_4&q_4&r_4&r_5\\p_5&q_5&r_5&s_5\end{bmatrix}\begin{bmatrix}\lambda_2\\\lambda_3\\\lambda_4\\\lambda_5\end{bmatrix} \qquad (39)
$$

where

$$
\begin{aligned}
p_2&=\frac{h_{x0}^2}{2\Delta\theta}+\frac{1}{\Delta\theta}\sum_{n=1}^{\infty}\left(h_{xa}^2+h_{xb}^2\right)+\frac{j_{y0}^2}{2\Delta\theta}+\frac{1}{\Delta\theta}\sum_{n=1}^{\infty}\left(j_{ya}^2+j_{yb}^2\right)\\
p_3&=\frac{h_{x0}k_{x0}}{2\Delta\theta}+\frac{1}{\Delta\theta}\sum_{n=1}^{\infty}(h_{xa}k_{xa}+h_{xb}k_{xb})+\frac{j_{y0}l_{y0}}{2\Delta\theta}\\
&\quad+\frac{1}{\Delta\theta}\sum_{n=1}^{\infty}(j_{ya}l_{ya}+j_{yb}l_{yb})\\
p_4&=\frac{j_{y0}m_{y0}}{2\Delta\theta}+\frac{1}{\Delta\theta}\sum_{n=1}^{\infty}(j_{ya}m_{ya}+j_{yb}m_{yb})\\
p_5&=\frac{h_{x0}n_{x0}}{2\Delta\theta}+\frac{1}{\Delta\theta}\sum_{n=1}^{\infty}(h_{xa}n_{xa}+h_{xb}n_{xb})+\frac{j_{y0}p_{y0}}{2\Delta\theta}\\
&\quad+\frac{1}{\Delta\theta}\sum_{n=1}^{\infty}(j_{ya}p_{ya}+j_{yb}p_{yb})\\
q_3&=\frac{k_{x0}^2}{2\Delta\theta}+\frac{1}{\Delta\theta}\sum_{n=1}^{\infty}\left(k_{xa}^2+k_{xb}^2\right)+\frac{l_{y0}^2}{2\Delta\theta}+\frac{1}{\Delta\theta}\sum_{n=1}^{\infty}\left(l_{ya}^2+l_{yb}^2\right)\\
q_4&=\frac{l_{y0}m_{y0}}{2\Delta\theta}+\frac{1}{\Delta\theta}\sum_{n=1}^{\infty}(l_{ya}m_{ya}+l_{yb}m_{yb})\\
q_5&=\frac{k_{x0}n_{x0}}{2\Delta\theta}+\frac{1}{\Delta\theta}\sum_{n=1}^{\infty}(k_{xa}n_{xa}+k_{xb}n_{xb})+\frac{l_{y0}p_{y0}}{2\Delta\theta}\\
&\quad+\frac{1}{\Delta\theta}\sum_{n=1}^{\infty}(l_{ya}p_{ya}+l_{yb}p_{yb})\\
r_4&=\frac{m_{y0}^2}{2\Delta\theta}+\frac{1}{\Delta\theta}\sum_{n=1}^{\infty}\left(m_{ya}^2+m_{yb}^2\right)\\
r_5&=\frac{m_{y0}p_{y0}}{2\Delta\theta}+\frac{1}{\Delta\theta}\sum_{n=1}^{\infty}(m_{ya}p_{ya}+m_{yb}p_{yb})\\
s_5&=\frac{n_{x0}^2}{2\Delta\theta}+\frac{1}{\Delta\theta}\sum_{n=1}^{\infty}\left(n_{xa}^2+n_{xb}^2\right)+\frac{p_{y0}^2}{2\Delta\theta}+\frac{1}{\Delta\theta}\sum_{n=1}^{\infty}\left(p_{ya}^2+p_{yb}^2\right)
\end{aligned}
$$

They can be transformed into this simple closed form by Parseval's theorem:

$$
\begin{aligned}
p_2&=\frac{\Gamma^6}{2}\left[A_3(\theta_F)+3B_1(\theta_F)+2B_2(\theta_F)+B_5(\theta_F)\right]\\
p_3&=\frac{\Gamma^6}{2}\left[2B_2(\theta_F)+6C_2(\theta_F)\right]\\
p_4&=-\frac{\Gamma^6}{2}\left[eA_2(\theta_F)+2A_4(\theta_F)\right]\\
p_5&=\frac{\Gamma^6}{2}\left[A_2(\theta_F)+2B_3(\theta_F)\right]\\
q_3&=\frac{\Gamma^6}{2}\left[4A_1(\theta_F)+4A_3(\theta_F)-12eB_4(\theta_F)+9e^2C_3(\theta_F)\right.\\
&\quad\left.+9E_1(\theta_F)\right]\\
q_4&=-\frac{3\Gamma^6}{2}C_4(\theta_F)\\
q_5&=\frac{\Gamma^6}{2}\left[-2B_3(\theta_F)+3eC_5(\theta_F)+3C_6(\theta_F)+3D_1(\theta_F)\right]\\
r_4&=\frac{\Gamma^6}{2}\left[A_1(\theta_F)+A_3(\theta_F)\right],\qquad r_5=-\frac{\Gamma^6}{2}\left[A_5(\theta_F)+B_2(\theta_F)\right]\\
s_5&=\frac{\Gamma^6}{2}\left[A_1(\theta_F)+B_1(\theta_F)+eB_2(\theta_F)+3B_5(\theta_F)\right] \qquad (40)
\end{aligned}
$$

where A_1, A_2, etc., are given in Appendix B. For example, $A_1(\theta_F)=\int_{\theta_0}^{\theta_F}\frac{\cos^2\tau}{\rho(\tau)^6}\,d\tau$. Note that p_2, p_3, p_4, etc., are all constants. Then, from Eq. (39) we get the values of the Lagrange multipliers:

$$
\begin{bmatrix}\lambda_2\\\lambda_3\\\lambda_4\\\lambda_5\end{bmatrix}=\begin{bmatrix}p_2&p_3&p_4&p_5\\p_3&q_3&q_4&q_5\\p_4&q_4&r_4&r_5\\p_5&q_5&r_5&s_5\end{bmatrix}^{-1}\begin{bmatrix}I_2\\I_3\\I_4\\I_5\end{bmatrix}
$$

When we express T_x and T_y using the above Lagrange multipliers, the following equations are obtained:

$$
\begin{aligned}
T_x(\theta) &= \frac{a_{x0}}{2} + \sum_{n=1}^{\infty} a_{xn}\cos\left(\frac{2n\pi}{\Delta\theta}\theta\right) + \sum_{n=1}^{\infty} b_{xn}\sin\left(\frac{2n\pi}{\Delta\theta}\theta\right) \\
&= \frac{1}{2\Delta\theta}(\lambda_2 h_{x0} + \lambda_3 k_{x0} + \lambda_5 n_{x0}) \\
&\quad + \frac{1}{\Delta\theta}\sum_{n=1}^{\infty}(\lambda_2 h_{xa} + \lambda_3 k_{xa} + \lambda_5 n_{xa})\cos\left(\frac{2n\pi}{\Delta\theta}\theta\right) \\
&\quad + \frac{1}{\Delta\theta}\sum_{n=1}^{\infty}(\lambda_2 h_{xb} + \lambda_3 k_{xb} + \lambda_5 n_{xb})\sin\left(\frac{2n\pi}{\Delta\theta}\theta\right) \qquad (41a)
\end{aligned}
$$

$$
\begin{aligned}
T_y(\theta) &= \frac{a_{y0}}{2} + \sum_{n=1}^{\infty} a_{yn}\cos\left(\frac{2n\pi}{\Delta\theta}\theta\right) + \sum_{n=1}^{\infty} b_{yn}\sin\left(\frac{2n\pi}{\Delta\theta}\theta\right) \\
&= \frac{1}{2\Delta\theta}(\lambda_2 j_{y0} + \lambda_3 l_{y0} + \lambda_4 m_{y0} + \lambda_5 p_{y0}) \\
&\quad + \frac{1}{\Delta\theta}\sum_{n=1}^{\infty}(\lambda_2 j_{ya} + \lambda_3 l_{ya} + \lambda_4 m_{ya} + \lambda_5 p_{ya}) \\
&\quad \times \cos\left(\frac{2n\pi}{\Delta\theta}\theta\right) \\
&\quad + \frac{1}{\Delta\theta}\sum_{n=1}^{\infty}(\lambda_2 j_{yb} + \lambda_3 l_{yb} + \lambda_4 m_{yb} + \lambda_5 p_{yb}) \\
&\quad \times \sin\left(\frac{2n\pi}{\Delta\theta}\theta\right) \qquad (41b)
\end{aligned}
$$

Eqs. (41a) and (41b) can be simplified into the following closed form by Parseval's theorem:

$$
\begin{aligned}
T_x(\theta) &= \frac{\Gamma^3}{2}\left[\frac{-\lambda_2\rho(\theta)\cos\theta + \lambda_3(3e\rho(\theta)\sin\theta K(\theta) - 2)}{(1+e\cos\theta)^3}\right. \\
&\quad \left. + \frac{\lambda_5\rho(\theta)\sin\theta}{(1+e\cos\theta)^3}\right] \qquad (42a)
\end{aligned}
$$

$$
\begin{aligned}
T_y(\theta) &= \frac{\Gamma^3}{2}\left[\frac{\lambda_2\sin\theta(1+\rho(\theta)) + 3\lambda_3\rho(\theta)^2 K(\theta) - \lambda_4}{(1+e\cos\theta)^3}\right. \\
&\quad \left. + \frac{\lambda_5\cos\theta(1+\rho(\theta))}{(1+e\cos\theta)^3}\right] \qquad (42b)
\end{aligned}
$$

Eqs. (42a) and (42b) are the final results for $T_x(\theta)$ and $T_y(\theta)$, which are the x- and y-components of thrust for the optimal reconfiguration of satellites in an elliptic orbit. Thus, we have obtained the optimal thrust functions in terms of the true anomaly. The performance index (21b) can then also be succinctly expressed as:

$$
J_{xy} = \frac{1}{2}(I_2\lambda_2 + I_3\lambda_3 + I_4\lambda_4 + I_5\lambda_5) \qquad (43)
$$

Furthermore, substituting Eqs. (42a) and (42b) into Eq. (34) yields

$$
\begin{aligned}
I_2(\theta) &= \frac{\Gamma^6}{2}\big[\lambda_2(A_3 + 3B_1 + eB_2 + B_5) + \lambda_3(2B_2 + 6C_2) \\
&\quad - \lambda_4(eA_2 + 2A_4) + \lambda_5(A_2 + 2B_3)\big] \\
I_3(\theta) &= \frac{\Gamma^6}{2}\big[\lambda_2(2B_2 + 6C_2) \\
&\quad + \lambda_3(4A_1 + 4A_3 - 12eB_4 + 9e^2C_3 + 9E_1) \\
&\quad - 3\lambda_4 C_4 + \lambda_5(-2B_3 + 3eC_5 + 3C_6 + 3D_1)\big] \\
I_4(\theta) &= -\frac{\Gamma^6}{2}\big[\lambda_2(eA_2 + 2A_4) + 3\lambda_3 C_4 - \lambda_4(A_1 + A_3) \\
&\quad + \lambda_5(A_5 + B_2)\big] \\
I_5(\theta) &= \frac{\Gamma^6}{2}\big[\lambda_2(A_2 + 2B_3) \\
&\quad + \lambda_3(-2eA_2 - 2A_4 + 3eC_5 + 3C_6 + 3D_1) \\
&\quad - \lambda_4(A_5 + B_2) + \lambda_5(A_1 + B_1 + eB_2 + 3B_5)\big]
\end{aligned}
$$

$$
\begin{bmatrix} Q_2(\theta) \\ Q_3(\theta) \\ Q_4(\theta) \\ Q_5(\theta) \end{bmatrix} = \frac{1}{1-e^2}\begin{bmatrix} -e & 1 & 0 & 0 \\ 1 & -e & 0 & 0 \\ 0 & 0 & -e & 1 \\ 0 & 0 & 1 & -e \end{bmatrix}\begin{bmatrix} I_2(\theta) \\ I_3(\theta) \\ I_4(\theta) \\ I_5(\theta) \end{bmatrix} \qquad (44)
$$

For A_1, A_2, etc., see Appendix B. Then, the x–y components of the positions and velocities during the maneuver will be

$$
\begin{bmatrix} \tilde{x}_p(\theta) \\ \tilde{x}'_p(\theta) \\ \tilde{y}_p(\theta) \\ \tilde{y}'_p(\theta) \end{bmatrix} = \begin{bmatrix} 0 & -s & -c & 3esK - 2 \\ 0 & -s' & -c' & 3e(s'K + s/\rho^2) \\ 1 & -c(1+1/\rho) & s(1+1/\rho) & 3\rho^2 K \\ 0 & 2s & 2c - e & 3(1 - 2esK) \end{bmatrix} \times \begin{bmatrix} Q_2(\theta) \\ Q_3(\theta) \\ Q_4(\theta) \\ Q_5(\theta) \end{bmatrix} \qquad (16)
$$

and the actual positions and velocities of x and y are

$$
\begin{aligned}
&\begin{bmatrix} x_p(\theta) \\ \dot{x}_p(\theta) \\ y_p(\theta) \\ \dot{y}_p(\theta) \end{bmatrix} \\
&= \begin{bmatrix} \frac{\Gamma}{\rho(\theta)} & 0 & 0 & 0 \\ \frac{e\sin\theta}{\Gamma} & \frac{\rho(\theta)}{\Gamma} & 0 & 0 \\ 0 & 0 & \frac{\Gamma}{\rho(\theta)} & 0 \\ 0 & 0 & \frac{e\sin\theta}{\Gamma} & \frac{\rho(\theta)}{\Gamma} \end{bmatrix}\begin{bmatrix} \tilde{x}_p(\theta) \\ \tilde{x}'_p(\theta) \\ \tilde{y}_p(\theta) \\ \tilde{y}'_p(\theta) \end{bmatrix} \\
&= \begin{bmatrix} 0 & -\Gamma\sin\theta & -\Gamma\cos\theta & \Gamma(3e\sin\theta K - \frac{2}{\rho}) \\ 0 & -\frac{\cos\theta}{\Gamma}\rho^2 & \frac{\sin\theta}{\Gamma}\rho^2 & \frac{e}{\Gamma}(\sin\theta + 3\rho^2\cos\theta K) \\ \frac{\Gamma}{\rho} & -\Gamma\cos\theta(1+\frac{1}{\rho}) & \Gamma\sin\theta(1+\frac{1}{\rho}) & 3\Gamma\rho K \\ \frac{e\sin\theta}{\Gamma} & \frac{\sin\theta}{\Gamma}(1+\rho^2) & \frac{1}{\Gamma}(e+\cos\theta(1+\rho^2)) & \frac{3}{\Gamma}\rho(1 - e\sin\theta\rho K) \end{bmatrix} \\
&\quad \times \begin{bmatrix} Q_2(\theta) \\ Q_3(\theta) \\ Q_4(\theta) \\ Q_5(\theta) \end{bmatrix} \qquad (45)
\end{aligned}
$$

We can find the x–y components of the Deputy's position and velocity during the maneuver by adding the particular solutions (Eq. (45)) to the homogeneous solutions (Eq. (15b)). These values are useful when evaluating the numerical simulation. Furthermore, it can be shown that when $e = 0$ Eqs. (42a) and (42b) are converged into Palmer's results (Eqs. (44) and (45) in [8]).

5. Applications

We have derived all the equations for analytical solution to the reconfiguration of satellite formation using thrust acceleration. Let us summarize the main steps.

(1) The relative dynamics in arbitrary elliptic orbit are described by Eqs. (5a) and (5b), which show the in-plane motion and the out-of-plane motion, respectively.
(2) The solution to out-of-plane dynamics (Eq. (5b)) is found to consist of the homogeneous solution (Eq. (10a)) and the particular solution (Eqs. (11a) and (11b)). The solution to in-plane dynamics (Eq. (5a)) is also found by adding the homogeneous solution (Eq. (15a)) to the particular solution (Eq. (16)).

(3) Thrust acceleration for the particular solutions is formulated in a Fourier series. To minimize fuel consumption and satisfy the constraints induced from initial and final boundary conditions, appropriate Fourier coefficients are determined. Based on the coefficients, the closed-form solutions for thrust acceleration are derived for the x-component of acceleration (Eq. (42a)), along with the y-component (Eq. (42b)) and z-component (Eq. (30)).
(4) The position and velocity of the Deputy satellite during the reconfiguration maneuvers are also derived in closed forms. Eqs. (10b) and (33) are for the z-component of the position and velocity, whereas Eqs. (15b) and (45) are for the x- and y-component of the position and velocity.
(5) The performance index can be also represented in a simple closed form. Eq. (31) yields the performance index for the out-of-plane motion, whereas Eq. (43) gives the performance index for the in-plane motion.

5.1. Sample problems

To validate the results of the analytical solution mentioned above, numerical simulations are carried out. We consider the reconfiguration problems of formation flying having periodic conditions where the Chief moves in a reference orbit of eccentricities, $e = 0, 0.1$, and 0.7, respectively. The numerical solutions are obtained with a general purpose optimization code, the Sparse Optimal Control Software (SOCS) [1]. SOCS solves the optimal control problem using a direct transcription method by which the dynamic system is converted into a problem with a finite set of variables and utilizes the mesh refinement algorithm to improve the accuracy of the discretization. SOCS then determines numerical solutions using sequential quadratic programming.

First, let us consider the case of $e = 0$, in which the Deputy is in a projected circular formation. The semi-major axis of the Chief's orbit is $a = 7 \times 10^6$ m. The formation is required to change its radius to from 500 m to 1000 m during one period of the reference orbit. Second, for the cases of $e = 0.1$ and 0.7, the initial and final states were determined by Eq. (46) to obtain a periodic condition [6]:

$$y'(0)/x(0) = -\left[(2+e)/(1+e)\right] \tag{46}$$

Eq. (46) expresses the relation between $y'(0)$ and $x(0)$ in the true anomaly domain. Therefore, 0 means that the Chief is located at the perigee of the reference orbit, and the semi-major axes of the Chief's orbits are $a = 7.78 \times 10^6$ m for $e = 0.1$ and $a = 2.33 \times 10^7$ m for $e = 0.7$, respectively. These values are chosen because we want to fix the distance to a perigee by $r_p = 7 \times 10^6$ m, and the identity $r_p = a(1-e)$ is used. In the case of $e = 0$, three Deputy satellites are simulated simultaneously, and the phase angle between them is 120°. The initial and final conditions of each satellite are given in Table 1. However, in the non-circular-orbit cases, only one satellite is simulated, because it is difficult or seems to be impossible to find the initial conditions for multi-satellite reconfiguration in the same relative orbit plane. The initial and final conditions of one satellite in each eccentricity ($e = 0.1$ and 0.7) are given in Table 2. Also, discretization method and the numbers of nodes through mesh refinement algorithm by SOCS are given in Table 3.

Fig. 2 shows the 3-dimensional trajectories in the local coordinate frame for the cases of each eccentricity. The trajectories in the x- and y-components are obtained from the sum of Eqs. (15b) and (45) and the trajectories in the z-component are obtained from the sum of Eqs. (10b) and (33). These trajectories generated by the analytical solutions are identical to the trajectories produced by the numerical tool, SOCS, where the same performance index (Eq. (18)) is used for SOCS. Fig. 3 demonstrates thrust profiles as a function of true anomaly using the analytical solutions (Eqs. (30), (42a), and (42b)). For the case when $e = 0$, the thrust profile of satellite 1 among the three satellites is depicted. In addition, Fig. 4 shows the differences of thrust profiles between the analytical solutions and numerical solutions from SOCS. Thrust accelerations from the analytical method are coincident with those obtained numerically within 0.02% error. Given in Table 4 is a comparison of the performance indices resulting from the analytical method (Eqs. (31) and (43)) with those from numerical tool, SOCS. The analytical results are found be same as those obtained by the numerical method.

Table 1
Initial and final conditions of three Deputy satellites for the formation case of $e = 0$.

	Initial conditions			Final conditions		
	Sat 1	Sat 2	Sat 3	Sat 1	Sat 2	Sat 3
x, m	250.00	−125.00	−125.00	500.00	−250.00	−250.00
$\dot{x}$, m s^{-1}	0.00	−0.23	0.23	0.00	−0.47	0.467
y, m	0.00	−433.01	433.01	0.00	−866.03	866.03
$\dot{y}$, m s^{-1}	−0.54	0.27	0.27	−1.08	0.54	0.54
z, m	500.00	−250.00	−250.00	1000.00	−500.00	−500.00
$\dot{z}$, m s^{-1}	0.00	−0.47	0.47	0.00	−0.93	0.93

Table 2
Initial and final conditions of one Deputy satellite for the formations cases of $e = 0.1$ and 0.7.

	Initial conditions		Final conditions	
	$e = 0.1$	$e = 0.7$	$e = 0.1$	$e = 0.7$
x, m	250.00	250.00	500.00	500.00
$\dot{x}$, m s^{-1}	0.00	0.00	0.00	0.00
y, m	0.00	0.00	0.00	0.00
$\dot{y}$, m s^{-1}	−0.54	−0.56	−1.08	−1.12
z, m	500.00	500.00	1000.00	1000.00
$\dot{z}$, m s^{-1}	0.00	0.00	0.00	0.00

Table 3
Summary of SOCS results.

	$e = 0$	$e = 0.1$	$e = 0.7$
Discretization method	Trapezoidal	Trapezoidal	Trapezoidal
# of nodes	113	135	225

6. Conclusion

This paper derives novel closed-form solutions to the reconfiguration of satellite formation in an arbitrary elliptic orbit. The thrust accelerations are low level, continuous and of variable magnitude. The analytical solution represents thrust accelerations minimizing fuel consumption. For given initial and desired relative positions of a Deputy satellite, we are able to immediately generate an appropriate thrust acceleration and reconfiguration trajectory in a closed form. The analytic solutions have no singularities and are valid for an arbitrary elliptic orbit with $0 < e < 1$ as well as for a circular orbit. It is simple to apply the results because the solutions are in closed forms. The solutions can be applied to any value of eccentricity for a Chief satellite because the solutions have no approximation on eccentricity. Additional Deputy satellites do not need any further analysis or computation because the analytic solutions require only given initial and desired final satellite positions. This paper also provides examples that show its use in the reconfiguration of satellite formation flying in an elliptic orbit, and the obtained analytical solutions are very consistent with numerical results.

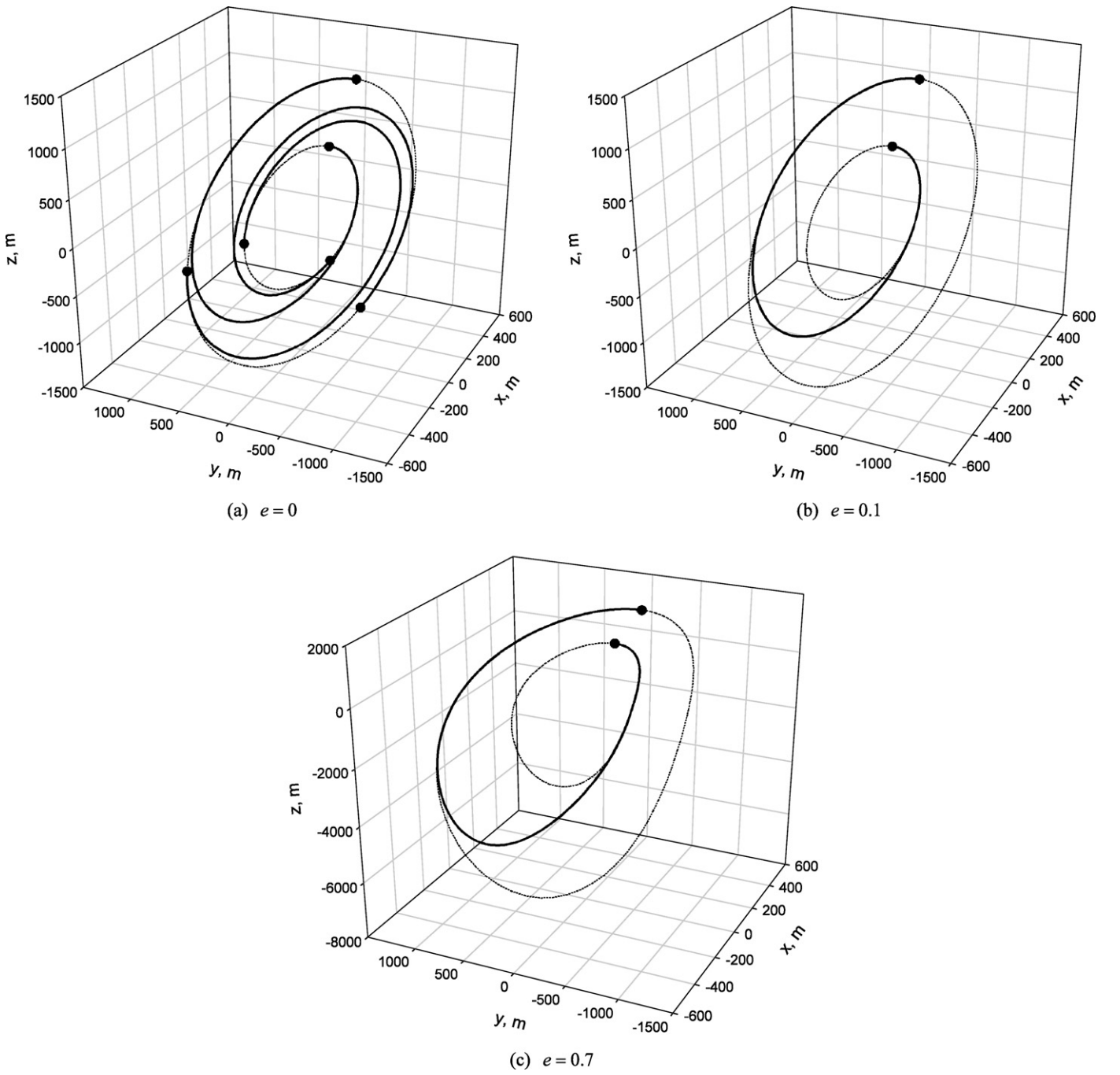

Fig. 2. The reconfiguration trajectories for the Deputy satellites.

Table 4
Comparison of performance indices for the analytical solution and the numerical solutions from SOCS.

	$e = 0$ (Satellite 1)	$e = 0.1$	$e = 0.7$
Analytical solution, $m^2\,s^{-4}$	1.1284095E−7	7.2363741E−8	4.6213681E−10
SOCS, $m^2\,s^{-4}$	1.1284096E−7	7.2363742E−8	4.6213685E−10

Acknowledgements

This work was supported by the Korea Science and Engineering Foundation (KOSEF) through the National Research Lab. Program funded by the Ministry of Science and Technology (No. M10600000282-06J0000-28210).

Appendix A. The inverse of $\boldsymbol{\Phi}_{\mathbf{xy}}(\theta)$

$$\boldsymbol{\Phi}_{\mathbf{xy}}^{-1}(\theta) = \begin{bmatrix} 0 & -s & -c & 3esK-2 \\ 0 & -s' & -c' & 3e(s'K+s/\rho^2) \\ 1 & -c(1+1/\rho) & s(1+1/\rho) & 3\rho^2 K \\ 0 & 2s & 2c-e & 3(1-2esK) \end{bmatrix}^{-1} = \begin{bmatrix} P_{11} & P_{12} & P_{13} & P_{14} \\ P_{21} & P_{22} & P_{23} & P_{24} \\ P_{31} & P_{32} & P_{33} & P_{34} \\ P_{41} & P_{42} & P_{43} & P_{44} \end{bmatrix}$$

where

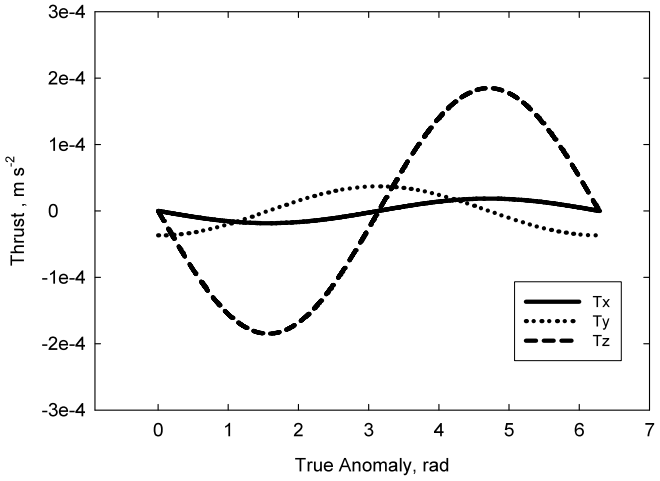

(a) $e = 0$ (satellite 1)

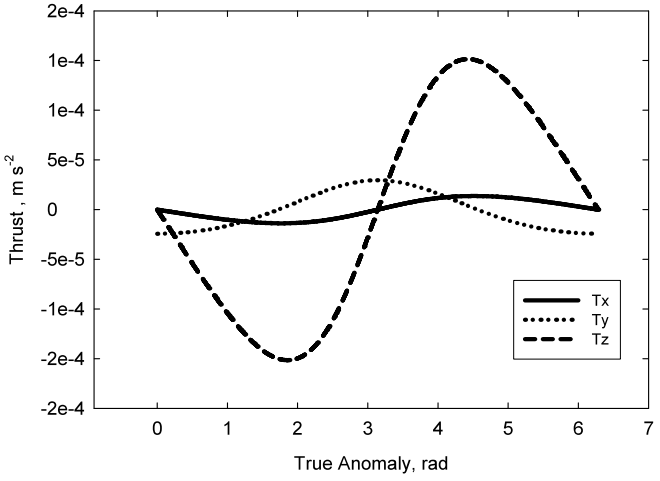

(b) $e = 0.1$

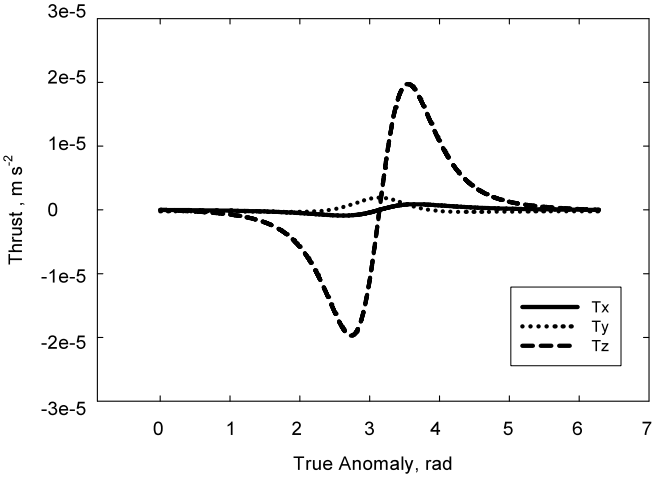

(c) $e = 0.7$

Fig. 3. Thrust profiles as the function of true anomaly using the analytical solutions for the reconfigurations shown in Fig. 2.

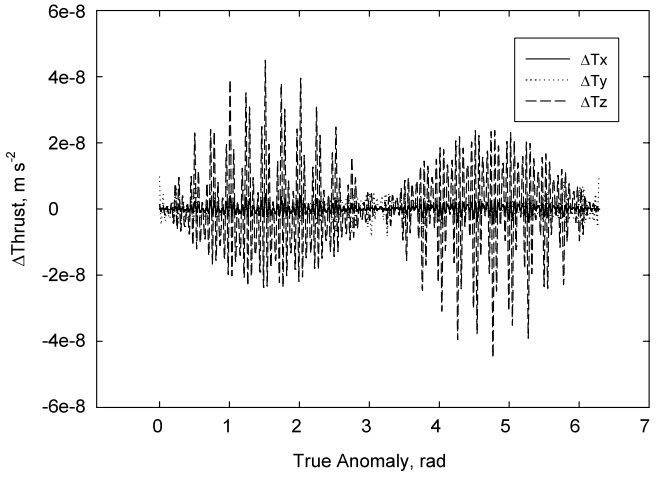

(a) $e = 0$ (Satellite 1)

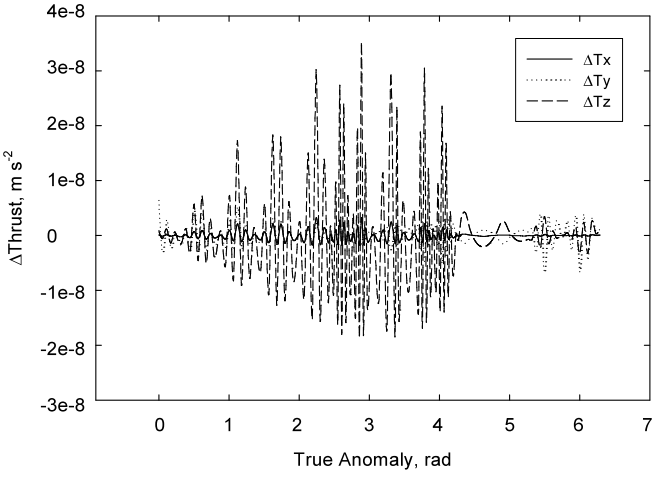

(b) $e = 0.1$

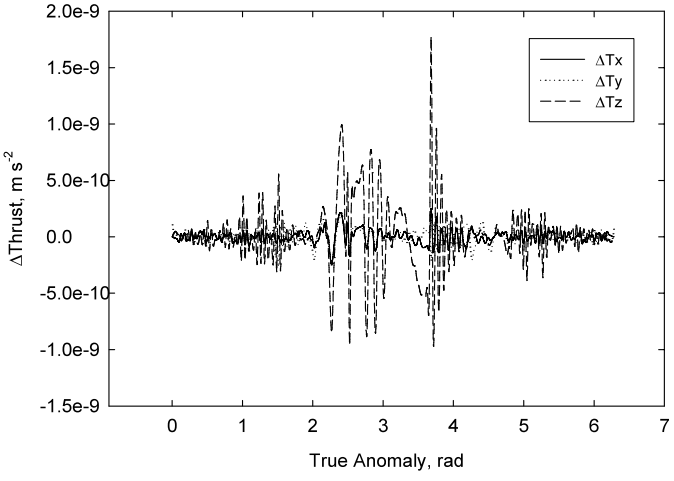

(c) $e = 0.7$

Fig. 4. The differences of thrust profiles between the analytical solutions (Fig. 3) and the numerical solutions from SOCS.

$$P_{11} = \frac{(9\rho + 3e^2 - 3)K - 3e\sin\theta\frac{1+\rho}{\rho}}{1-e^2}$$

$$P_{12} = \frac{3e\rho\sin\theta K + (\rho+1)(\rho-2)}{1-e^2}, \qquad P_{13} = 1$$

$$P_{14} = \frac{3\rho^2 K - e\sin\theta(1+\rho)}{1-e^2}$$

$$P_{21} = \frac{3\sin\theta(1+\frac{e^2}{\rho}) - 3e(3\rho + e^2 - 1)K}{1-e^2}$$

$$P_{22} = \frac{2e - \rho\cos\theta - 3e^2\rho\sin\theta K}{1-e^2}, \qquad P_{23} = 0$$

$$P_{24} = \frac{\sin\theta(1+\rho) - 3e\rho^2 K}{1-e^2}, \qquad P_{31} = \frac{3(e+\cos\theta)}{1-e^2}$$

$$P_{32} = \frac{\rho\sin\theta}{1-e^2}, \qquad P_{33} = 0$$

$$P_{34} = \frac{e + \cos\theta(1+\rho)}{1-e^2}, \qquad P_{41} = \frac{1-e^2-3\rho}{1-e^2}$$

$$P_{42} = -\frac{e\rho\sin\theta}{1-e^2}, \qquad P_{43} = 0, \qquad P_{44} = -\frac{\rho^2}{1-e^2}$$

Appendix B. Integration results

Here, following identities [13] are useful. (E denotes an eccentric anomaly.)

$$d\theta = \frac{(1-e^2)^{1/2}}{1-e\cos E}\,\mathrm{d}E, \qquad \rho(\theta) = 1 + e\cos\theta = \frac{1-e^2}{1-e\cos E}$$

$$K(\theta) = \left(1-e^2\right)^{-3/2}[E - e\sin E - M_0]$$

(where $M_0 \equiv E_0 - e\sin E_0$)

$$\cos\theta = \frac{\cos E - e}{1-e\cos E}, \qquad \sin\theta = \frac{(1-e^2)^{1/2}\sin E}{1-e\cos E}$$

Also, with the definition $S(\cdot) = S[\cdot(\theta)] = \int_{\theta_0}^{\theta} \cdot(\tau)\,\mathrm{d}\tau$, the following is frequently used:

$$A_1 = S\left[\frac{\cos^2\theta}{\rho^6}\right]$$
$$= \left(1-e^2\right)^{-11/2}\left[-\frac{1}{80}e^3\sin 5E + \frac{1}{32}e^2\left(2e^2+3\right)\sin 4E\right.$$
$$-\frac{1}{8}e\left(6e^4+65e^2+34\right)\sin E$$
$$-\frac{1}{48}e\left(4e^4+29e^2+12\right)\sin 3E + \frac{1}{8}\left(18e^4+41e^2+4\right)E$$
$$\left.+\frac{1}{4}\left(5e^4+9e^2+1\right)\sin 2E\right]_{\theta_0}^{\theta}$$

$$A_2 = S\left[\frac{\sin\theta\cos\theta}{\rho^6}\right]$$
$$= \left(1-e^2\right)^{-5}\left[\frac{1}{80}e^3\cos 5E - \frac{1}{32}e^2\left(e^2+3\right)\cos 4E\right.$$
$$+\frac{7}{8}e\left(e^2+2\right)\cos E + \frac{1}{16}e\left(5e^2+4\right)\cos 3E$$
$$\left.-\frac{1}{8}\left(e^4+9e^2+2\right)\cos 2E\right]_{\theta_0}^{\theta}$$

$$A_3 = S\left[\frac{\sin^2\theta}{\rho^6}\right]$$
$$= \left(1-e^2\right)^{-9/2}\left[\frac{1}{80}e^3\sin 5E - \frac{3}{32}e^2\sin 4E\right.$$
$$-\frac{1}{8}e\left(e^2+6\right)\sin E + \frac{1}{48}e\left(e^2+12\right)\sin 3E$$
$$\left.+\frac{1}{8}\left(3e^2+4\right)E - \frac{1}{4}\sin 2E\right]_{\theta_0}^{\theta}$$

$$A_4 = S\left[\frac{\sin\theta}{\rho^6}\right]$$
$$= \left(1-e^2\right)^{-5}\left[-\frac{1}{80}e^4\cos 5E + \frac{1}{8}e^3\cos 4E\right.$$
$$-\frac{1}{16}e^2\left(e^2+8\right)\cos 3E + \frac{1}{2}e\left(e^2+2\right)\cos 2E$$
$$\left.-\frac{1}{8}\left(e^4+12e^2+8\right)\cos E\right]_{\theta_0}^{\theta}$$

$$A_5 = A_1 + A_3 = S\left[\frac{\cos\theta}{\rho^6}\right]$$
$$= \left(1-e^2\right)^{-11/2}\left[\frac{1}{80}e^4\sin 5E - \frac{1}{32}e^3\left(e^2+4\right)\sin 4E\right.$$
$$+\frac{1}{16}e^2\left(7e^2+8\right)\sin 3E - \frac{3}{8}e\left(e^4+12e^2+8\right)E$$
$$\left.-\frac{1}{4}e\left(e^4+10e^2+4\right)\sin 2E + \frac{1}{8}\left(29e^4+68e^2+8\right)\sin E\right]_{\theta_0}^{\theta}$$

$$B_1 = S\left[\frac{\sin^2\theta}{\rho^5}\right]$$
$$= \left(1-e^2\right)^{-7/2}\left[-\frac{1}{32}e^2\sin 4E - \frac{1}{2}e\sin E + \frac{1}{6}e\sin 3E\right.$$
$$\left.+\frac{1}{8}\left(e^2+4\right)E - \frac{1}{4}\sin 2E\right]_{\theta_0}^{\theta}$$

$$B_2 = S\left[\frac{\cos\theta}{\rho^5}\right]$$
$$= \left(1-e^2\right)^{-9/2}\left[-\frac{1}{32}e^3\sin 4E + \frac{1}{12}e^2\left(e^2+3\right)\sin 3E\right.$$
$$-\frac{5}{8}e\left(3e^2+4\right)E - \frac{1}{4}e\left(4e^2+3\right)\sin 2E$$
$$\left.+\frac{1}{4}\left(3e^4+21e^2+4\right)\sin E\right]_{\theta_0}^{\theta}$$

$$B_3 = eA_2 + A_4 = S\left[\frac{\sin\theta\cos\theta}{\rho^5}\right]$$
$$= \left(1-e^2\right)^{-4}\left[-\frac{1}{32}e^2\cos 4E + \frac{1}{4}e\left(e^2+6\right)\cos E\right.$$
$$\left.+\frac{1}{12}e\left(e^2+2\right)\cos 3E - \frac{1}{8}\left(5e^2+2\right)\cos 2E\right]_{\theta_0}^{\theta}$$

$$B_4 = S\left[\frac{\sin\theta K}{\rho^5}\right]$$
$$= \left(1-e^2\right)^{-11/2}\left[-\frac{1}{80}e^4\sin 5E + \frac{1}{32}e^3(E-M_0)\cos 4E\right.$$
$$+\frac{11}{128}e^3\sin 4E - \frac{1}{4}e^2(E-M_0)\cos 3E$$
$$-\frac{1}{48}e^2\left(e^2+8\right)\sin 3E - \frac{1}{8}e\left(3e^2+4\right)E$$
$$-\frac{1}{4}\left(3e^2+4\right)(E-M_0)\cos E + \frac{1}{8}\left(e^3+6e\right)(E-M_0)\cos 2E$$
$$\left.+\frac{1}{8}\left(e^4+12e^2+8\right)\sin E - \frac{1}{16}(e^3+2e)\sin 2E\right]_{\theta_0}^{\theta}$$

$$
\begin{aligned}
B_5 &= S\left[\frac{\cos^2\theta}{\rho^5}\right] \\
&= \left(1-e^2\right)^{-9/2}\left[\frac{1}{32}e^2\sin 4E - \frac{7}{2}e\left(e^2+1\right)\sin E\right. \\
&\quad - \frac{1}{6}e\left(e^2+1\right)\sin 3E + \frac{1}{8}\left(4e^4+27e^2+4\right)E \\
&\quad \left. + \frac{1}{4}\left(e^4+5e^2+1\right)\sin 2E\right]_{\theta_0}^{\theta} \\
C_1 &= B_1 + eB_2 + B_6 = S\left[\frac{\sin\theta\cos\theta K}{\rho^4}\right] \\
&= \left(1-e^2\right)^{-9/2}\left[\frac{5}{8}e^2E - \frac{1}{32}e^2\sin 4E + \frac{5}{4}e(E-M_0)\cos E\right. \\
&\quad + \frac{1}{12}e(E-M_0)\cos 3E - \frac{1}{4}\left(e^2+1\right)(E-M_0)\cos 2E \\
&\quad - \frac{1}{4}\left(e^3+6e\right)\sin E - \frac{1}{8}\left(e^2-1\right)\sin 2E \\
&\quad \left. + \frac{1}{36}(3e^3+2e)\sin 3E\right]_{\theta_0}^{\theta} \\
C_2 &= S\left[\frac{\sin\theta K}{\rho^4}\right] \\
&= \left(1-e^2\right)^{-9/2}\left[\frac{1}{32}e^3\sin 4E - \frac{1}{12}e^2(E-M_0)\cos 3E\right. \\
&\quad - \frac{5}{36}e^2\sin 3E - \frac{1}{8}e(e^2+4)E + \frac{1}{2}e(E-M_0)\cos 2E \\
&\quad \left. - \frac{1}{4}\left(e^2+4\right)(E-M_0)\cos E + \frac{1}{4}\left(3e^2+4\right)\sin E\right]_{\theta_0}^{\theta} \\
C_3 &= S\left[\frac{\sin^2\theta K^2}{\rho^4}\right] \\
&= \left(1-e^2\right)^{-11/2}\frac{1}{8640}\left[-1080e^3\sin E + 540e^3\sin 3E\right. \\
&\quad - 108e^3\sin 5E + 3240e^2E + 2160e^2M_0\cos 2E \\
&\quad - 2160e^2E\cos 2E - 540e^2M_0\cos 4E + 540e^2E\cos 4E \\
&\quad - 1080e^2\sin 2E + 135e^2\sin 4E - 8640eM_0\cos E \\
&\quad + 8640eE\cos E + 960eM_0\cos 3E - 960eE\cos 3E \\
&\quad - 2160eM_0^2\sin E - 2160eE^2\sin E + 4320eM_0E\sin E \\
&\quad - 8640e\sin E + 720eM_0^2\sin 3E + 720eE^2\sin 3E \\
&\quad - 1440eM_0E\sin 3E + 320e\sin 3E + 1440E^3 \\
&\quad - 4320M_0E^2 + 4320M_0^2E + 2160M_0\cos 2E \\
&\quad - 2160E\cos 2E - 2160M_0^2\sin 2E - 2160E^2\sin 2E \\
&\quad \left. + 4320M_0E\sin 2E + 1080\sin 2E\right]_{\theta_0}^{\theta} \\
C_4 &= S\left[\frac{K}{\rho^4}\right] \\
&= \left(1-e^2\right)^{-5}\left[-\frac{1}{32}e^4\cos 4E + \frac{2}{9}e^3\cos 3E\right. \\
&\quad - \frac{1}{12}e^3(E-M_0)\sin 3E - \frac{1}{8}e^2\left(e^2+3\right)\cos 2E \\
&\quad + \frac{3}{4}e^2(E-M_0)\sin 2E - 2e\cos E \\
&\quad + \frac{1}{4}\left(3e^2+2\right)(E-2M_0)E \\
&\quad \left. - \frac{3}{4}\left(e^3+4e\right)(E-M_0)\sin E\right]_{\theta_0}^{\theta}
\end{aligned}
$$

$$
\begin{aligned}
C_5 &= S\left[\frac{\sin^2\theta K}{\rho^4}\right] \\
&= \left(1-e^2\right)^{-4}\left[\frac{1}{32}e^2\cos 4E + \frac{1}{2}e\cos E - \frac{1}{18}e\cos 3E\right. \\
&\quad - \frac{1}{4}e(E-M_0)\sin E + \frac{1}{12}e(E-M_0)\sin 3E \\
&\quad + \frac{1}{4}E(E-2M_0) - \frac{1}{8}(e^2+1)\cos 2E \\
&\quad \left. - \frac{1}{4}(E-M_0)\sin 2E\right]_{\theta_0}^{\theta} \\
C_6 &= S\left[\frac{\cos\theta K}{\rho^4}\right] \\
&= \left(1-e^2\right)^{-5}\left[\frac{1}{2}e^3\cos 2E + \frac{1}{32}e^3\cos 4E\right. \\
&\quad - \frac{1}{36}e^2\left(3e^2+5\right)\cos 3E + \frac{1}{12}e^2(E-M_0)\sin 3E \\
&\quad - \frac{1}{4}\left(e^3+4e\right)E(E-2M_0) - \frac{1}{4}\left(e^4-5e^2-4\right)\cos E \\
&\quad + \frac{1}{4}\left(11e^2+4\right)(E-M_0)\sin E \\
&\quad \left. - \frac{1}{4}\left(e^3+2e\right)(E-M_0)\sin 2E\right]_{\theta_0}^{\theta} \\
D_1 &= eC_2 + C_3 = S\left[\frac{\cos\theta K}{\rho^3}\right] \\
&= \left(1-e^2\right)^{-4}\left[-\frac{1}{12}e^2\cos 3E - \frac{3}{4}eE(E-2M_0)\right. \\
&\quad - \frac{1}{4}e(E-M_0)\sin 2E - \frac{1}{4}\left(e^2-4\right)\cos E \\
&\quad \left. + \frac{1}{8}\left(2e^3+e\right)\cos 2E + \left(e^2+1\right)(E-M_0)\sin E\right]_{\theta_0}^{\theta} \\
E_1 &= S\left[\frac{K^2}{\rho^2}\right] \\
&= \left(1-e^2\right)^{-9/2}\left[\frac{1}{12}e^3\sin 3E - \frac{1}{2}e^2(E-M_0)\cos 2E\right. \\
&\quad - \frac{1}{4}e\left(e^2+4M_0^2+4E^2-8M_0E\right)\sin E \\
&\quad \left. + \frac{1}{6}E\left(3e^2+6M_0^2+2E^2-6M_0E\right)\right]_{\theta_0}^{\theta}
\end{aligned}
$$

Appendix C. The verification of Eq. (30) when $e = 0$

We will show Eq. (30) becomes Palmer's result (Eq. (30) in [8]) when $e = 0$. Hereafter barred ($\bar{}$) notations mean Palmer's values. In the case of $e = 0$, it is easy to show that

$$
\begin{aligned}
p_0 &= \frac{1}{4\bar{\Omega}^3}[\bar{\beta} + \sin\bar{\beta}\cos\bar{\beta}] \\
p_1 &= \frac{1}{4\bar{\Omega}^3}\sin^2\bar{\beta} \\
q_1 &= \frac{1}{4\bar{\Omega}^3}[\bar{\beta} - \sin\bar{\beta}\cos\bar{\beta}] \\
p_0q_1 - p_1^2 &= \frac{1}{16\bar{\Omega}^6}\left[\bar{\beta}^2 - \sin^2\bar{\beta}\right]
\end{aligned}
\tag{C.1}
$$

where $\overline{\Omega}$ is the constant orbital rate of the Chief satellite, $\overline{\beta} \equiv \overline{\Omega} t_F$, and t_F is the time when the thruster is switched off. Recollecting Eq. (22), we have

$$I_0 = \tilde{z}_p(\theta_F)\sin\theta_F + \tilde{z}'_p\cos\theta_F$$
$$I_1 = -\tilde{z}_p(\theta_F)\cos\theta_F + \tilde{z}'_p\sin\theta_F$$

With Palmer's notations,

$$\overline{I_0} = \overline{\Omega}(z_F - \hat{z}_F), \qquad \overline{I_1} = \dot{z}_F - \dot{\hat{z}}_F$$
$$\begin{bmatrix} \overline{K_0} \\ \overline{K_1} \end{bmatrix} = \begin{bmatrix} 1 & \cot(\overline{\beta}/2) \\ -\cot(\overline{\beta}/2) & 1 \end{bmatrix} \begin{bmatrix} \overline{I_0} \\ \overline{I_1} \end{bmatrix} \tag{C.2}$$

where $z_F \equiv z(t_F)$. Therefore, we obtain the following:

$$I_0 = \frac{\overline{I_0}}{\Gamma\overline{\Omega}}\sin\overline{\beta} + \Gamma\overline{I_1}\cos\overline{\beta}$$
$$I_1 = -\frac{\overline{I_0}}{\Gamma\overline{\Omega}}\cos\overline{\beta} + \Gamma\overline{I_1}\sin\overline{\beta} \tag{C.3}$$

Coalescing Eqs. (C.2) and (C.3) yields

$$\begin{aligned} I_0 &= \left[\frac{\sin\overline{\beta}}{\Gamma\overline{\Omega}}\sin^2\left(\frac{\overline{\beta}}{2}\right) + \Gamma\cos\overline{\beta}\sin\left(\frac{\overline{\beta}}{2}\right)\cos\left(\frac{\overline{\beta}}{2}\right)\right]\overline{K_0} \\ &\quad + \left[-\frac{\sin\overline{\beta}}{\Gamma\overline{\Omega}}\sin\left(\frac{\overline{\beta}}{2}\right)\cos\left(\frac{\overline{\beta}}{2}\right) + \Gamma\cos\overline{\beta}\sin^2\left(\frac{\overline{\beta}}{2}\right)\right]\overline{K_1} \\ I_1 &= \left[-\frac{\cos\overline{\beta}}{\Gamma\overline{\Omega}}\sin^2\left(\frac{\overline{\beta}}{2}\right) + \Gamma\sin\overline{\beta}\sin\left(\frac{\overline{\beta}}{2}\right)\cos\left(\frac{\overline{\beta}}{2}\right)\right]\overline{K_0} \\ &\quad + \left[\frac{\cos\overline{\beta}}{\Gamma\overline{\Omega}}\sin\left(\frac{\overline{\beta}}{2}\right)\cos\left(\frac{\overline{\beta}}{2}\right) + \Gamma\sin\overline{\beta}\sin^2\left(\frac{\overline{\beta}}{2}\right)\right]\overline{K_1} \end{aligned} \tag{C.4}$$

From Eq. (C.4),

$$\begin{aligned} \lambda_0 &= \frac{1}{p_0q_1 - p_1^2}[q_1I_0 - p_1I_1] \\ &= \frac{2\overline{\Omega}^2}{\Gamma}\frac{\sin\overline{\beta}}{\overline{\beta}+\sin\overline{\beta}}\overline{K_0} + \frac{2\overline{\Omega}^2}{\Gamma}\frac{\cos\overline{\beta}-1}{\overline{\beta}-\sin\overline{\beta}}\overline{K_1} \\ &= \frac{1}{\Gamma^3}\left[\bar{\lambda}_0\frac{\sin\overline{\beta}}{1-\cos\overline{\beta}} - \bar{\lambda}_1\right] \\ \lambda_1 &= \frac{1}{p_0q_1 - p_1^2}[-p_1I_0 + p_0I_1] \\ &= \frac{2\overline{\Omega}^2}{\Gamma}\frac{1-\cos\overline{\beta}}{\overline{\beta}+\sin\overline{\beta}}\overline{K_0} + \frac{2\overline{\Omega}^2}{\Gamma}\frac{\sin\overline{\beta}}{\overline{\beta}-\sin\overline{\beta}}\overline{K_1} \\ &= \frac{1}{\Gamma^3}\left[\bar{\lambda}_0 + \bar{\lambda}_1\frac{\sin\overline{\beta}}{1-\cos\overline{\beta}}\right] \end{aligned} \tag{C.5}$$

where $\Gamma^2\overline{\Omega} = 1$ for the circular reference orbit is used and the following is given in Eq. (28) of [8]:

$$\bar{\lambda}_0 = 2\overline{\Omega}\overline{K}_0\frac{1-\cos\overline{\beta}}{\overline{\beta}+\sin\overline{\beta}}, \qquad \bar{\lambda}_1 = 2\overline{\Omega}\overline{K}_1\frac{1-\cos\overline{\beta}}{\overline{\beta}-\sin\overline{\beta}}$$

Using the trigonometric identity, $\cot(\frac{\overline{\beta}}{2}) = \frac{\sin\overline{\beta}}{1-\cos\overline{\beta}}$, and $e = 0$ for the circular reference orbit, we finally have the optimal thrust acceleration from Eq. (30):

$$\begin{aligned} T_z &= \frac{\Gamma^3}{2}\left[\lambda_0\cos(\overline{\Omega}t) + \lambda_1\sin(\overline{\Omega}t)\right] \\ &= \left[\frac{\overline{\lambda_0}}{2}\cot\left(\frac{\overline{\beta}}{2}\right) - \frac{\overline{\lambda_1}}{2}\right]\cos(\overline{\Omega}t) + \left[\frac{\overline{\lambda_0}}{2} + \frac{\overline{\lambda_1}}{2}\cot\left(\frac{\overline{\beta}}{2}\right)\right]\sin(\overline{\Omega}t) \\ &= \overline{\Gamma}\cos(\overline{\Omega}t - \bar{\zeta}) \end{aligned} \tag{C.6}$$

where

$$\overline{\Gamma} = \frac{1}{2}\left|\csc\left(\frac{\overline{\beta}}{2}\right)\right|\sqrt{(\overline{\lambda_0}^2 + \overline{\lambda_1}^2)}, \qquad \bar{\zeta} = \bar{\upsilon} + \frac{\overline{\beta}}{2},$$
$$\overline{\lambda_1} = \overline{\lambda_0}\tan\bar{\upsilon}$$

Eq. (C.6) is exactly the same as Eq. (30) in [8], and this is the end of the proof.

References

[1] J.T. Betts, W.P. Huffman, Sparse Optimal Control Software, Ver. 6.4.1, The Boeing Co., Seattle, WA, July 2005.
[2] M.L. Boas, Mathematical Methods in the Physical Sciences, second ed., Wiley, New York, 1983, pp. 307–334.
[3] M.E. Campbell, Planning algorithm for multiple satellite clusters, Journal of Guidance, Control, and Dynamics 26 (5) (2003) 770–780.
[4] V.M. Guibout, D.J. Scheeres, Solving relative two-point boundary value problems: Spacecraft formation flight transfers application, Journal of Guidance, Control, and Dynamics 27 (4) (2004) 693–704.
[5] M. Humi, Fuel-optimal rendezvous in a general central force field, Journal of Guidance, Control, and Dynamics 16 (1) (1993) 215–217.
[6] G. Inalhan, M. Tillerson, J.P. How, Relative dynamics and control of spacecraft formations in eccentric orbits, Journal of Guidance, Control, and Dynamics 25 (1) (2002) 48–59.
[7] E.M.C. Kong, D.M. Miller, Optimal spacecraft reorientation for earth orbiting clusters: Applications to Techsat 21, Acta Astronautica 53 (2003) 863–877.
[8] P. Palmer, Optimal relocation of satellites flying in near-circular-orbit formations, Journal of Guidance, Control, and Dynamics 29 (3) (2006) 519–526.
[9] P. Sengupta, S.R. Vadali, Analytical solution for power-limited optimal rendezvous near an elliptic orbit, Journal of Optimization Theory and Applications 138 (1) (2008) 115–137.
[10] R. Sharma, P. Sengupta, S.R. Vadali, Near-optimal feedback rendezvous in elliptic orbits accounting for nonlinear differential gravity, Journal of Guidance, Control, and Dynamics 30 (6) (2007) 1803–1813.
[11] J. Tschauner, P. Hempel, Rendezvous with a target in an elliptical orbit, Acta Astronautica 11 (2) (1965) 104–109.
[12] S.S. Vaddi, K.T. Alfriend, S.R. Vadali, P. Sengupta, Formation establishment and reconfiguration using impulsive control, Journal of Guidance, Control, and Dynamics 28 (2) (2005) 262–268.
[13] D.A. Vallado, Fundamentals of Astrodynamics and Applications, Kluwer Academic Publishers, Boston, 2001, pp. 55–56.
[14] K. Yamanaka, F. Ankersen, New state transition matrix for relative motion on an arbitrary elliptical orbit, Journal of Guidance, Control, and Dynamics 25 (1) (2002) 60–66.
[15] G. Yang, Q. Yang, V. Kapila, D. Palmer, R. Vaidyanathan, Fuel optimal maneuvers for multiple spacecraft formation reconfiguration using multi-agent optimization, International Journal of Robust and Nonlinear Control (2002) 243–283.
[16] D. Zanon, M.E. Campbell, Optimal planner for spacecraft formations in elliptical orbits, Journal of Guidance, Control, and Dynamics 29 (1) (2006) 161–171.